Review by Anonymous Referee #1 & author's response

This study implemented Miscanthus into JULES-BE based on site observations from Lincolnshire, UK and a global bioenergy yield dataset. Future simulation was conducted to evaluate the implication of explicit representation of bioenergy crops for climate mitigation. Three simulations were carried to demonstrate the utilization of the new harvesting scheme in JULE-BE.

Miscanthus is one of the most important perennial bioenergy crops that are proposed as biofuel feedstocks for climate mitigation purposes in future scenarios, in particular for the Shared Socio-economic Pathways (SSPs) of the Coupled Model Intercomparison Project Phase 6 (CMIP6). Given the projected biofuel expansion at a global scale, this study constitutes an important step to explicitly represent bioenergy crops in land surface modeling to assess the implications of large-scale bioenergy expansion on water and carbon cycling.

However, there are a number of suggested comments that should be addressed prior to acceptance. For example, model configurations were not well described. A sensitivity analysis is missing. More discussions on the mismatch between simulation and observation is in need.

My main concerns are:
Page 2, on line 10-15: Several ESMs have represented bioenergy crops. Therefore, it will be better to conclude and compare what has been implemented in other ESMs.

> This section discusses BE crops in ESMs under the general banner of "DGVMs". Adjusted the language in this paragraph to make this more specific. This now reads:
>
> "Dynamic global vegetation models (DGVMs), by contrast, are models specifically developed to address questions about large-scale vegetation patterns and productivity, and their links with the climate and Earth system (particularly as part of the Earth system models of which they form the terrestrial components) (Sitch et al., 2008). However, this typically occurs at the expense of representation of specific plant species and detailed site and management information. There are differences between DGVMs (and ESMs) in representation of bioenergy crops and calculation of harvests (Krause et al., 2018): although some feature explicit representation of bioenergy crops and harvesting (e.g. LPJml (Beringer et al., 2011;Boysen et al., 2016); ORCHIDEE-MICT-BIOENERGY (Li et al., 2018b)), others use approximations based on generic plant functional types (PFTs) and calculate harvests as a fixed proportion of productivity (e.g. NorESM (Muri, 2018))."

The methods section lacks description for model configuration. For example, it is not clear how the authors chose the initial conditions?

> Added this explanatory paragraph at the start of Section 2.5:
> "Simulations were carried out to evaluate and illustrate the new functionality in JULES-BE. These simulations were all based on the JULES-ES configuration, a set of options designed for best representation of carbon cycle and climate dynamics over decadal to centennial timescales. All simulations began with initial conditions from a spin-up to equilibrium, then included a transient spin-up period prior to the main run."

Page 5, line 24: Have you done any sensitivity analysis for the parameters?

PFT parameter choice is discussed in the Supplement and in Harper et al. (2018b).

Added this sentence to Section 2.4:
"(See also Harper et al. (2018b) for further information about PFT parameter selection.)"

Page 6, line 25: can you justify the consistency between the forcing used to drive the future simulation in this study and the forcing used to drive IMAGE 3.0 to generate the RCP2.6-SSP2 scenario?

The future simulation is driven by modelled meteorology from HadGEM2-ES, forced by the RCP2.6 concentrations of CO2 and other radiative forcing agents, and is therefore consistent with the IMAGE scenario of RCP2.6.

Added "(for RCP2.6)" to Page 6, line 26, to improve clarity.

Page 7, Line 25 and Figure 2, the simulated LAI is much lower than the observations, can you adjust some more parameters based on observations or add more discussions on the potential reasons?

Section 2.4 discusses PFT parametrisation, with further details provided in the Supplement. Leaf mass per area and leaf nitrogen concentration were taken from literature. Values for variables governing *vcmax* were determined via iteration to fit the GPP observations at this site. PFT allometry was optimised for height to above-ground biomass relationship.

Page 6, line 9: Only meteorological and soil properties data were mentioned. It will be great if the authors can also add some descriptions for the validation dataset here. For example, I can see it has some missing periods for the observed LAIs in Figure 1. And how about the land management practice for Miscanthus at this site? Why the durations for soil properties (2009-2010), meteorology (2006-2013), and model validation (2008-2013 for GPP, 2011-2013 for LAI) are inconsistent?

Added further detail to Section 2.5.1 for increased clarity. These paragraphs now read:

"Adjustment of PFT parameters for Miscanthus was performed using observational data collected from a commercial Miscanthus plantation in Lincolnshire, UK. The site is on a compacted loam soil previously used to grow wheat and oilseed rape. The site had mean annual temperature of 9.8 °C and mean annual precipitation of 621 mm. The net ecosystem exchange of CO2 was measured by eddy covariance methodology. Gross primary productivity (GPP) was calculated using the REddyProc method described by Robertson et al. (2017), after Reichstein et al. (2005). Manual measurements of height and LAI were taken over the growing season (Fig. 2). The site practices, harvesting regime and data collection are described by Robertson et al. (2016) and Robertson et al. (2017).

"JULES requires meteorological and soil ancillary (time-invariant) data to drive the model. Meteorological data were collected at the site on an hourly basis during 2006–2013 (shortwave and longwave radiation, wind speed, precipitation, temperature, air pressure, and specific humidity). Physical soil properties (soil albedo, heat capacity, thermal conductivity, hydraulic conductivity at saturation, soil moisture at saturation, soil moisture at critical point, soil moisture at wilting point, Brooks-Corey exponent for soil hydraulic calculations, soil matric suction at saturation) were derived from measurements taken at the site between 2009 and 2010."

Table 3: the authors listed parameters values for C4 grass and Miscanthus for comparison purposes. Can you add more results from C4 grass (e.g., GPP, LAI, NEE) to have a better sense of the difference between these two PFTs?

Added a Figure S3 to the Supplement showing GPP, NPP, height and LAI at the Lincolnshire site for Miscanthus and C4 grass.

Figure 2: why the modelled LAI maintained a very high value until the next year and then suddenly became zero (e.g., around Feb 2012)? Especially give GPP did not exhibit similar behaviors in Figure 3.

LAI is suddenly reduced to near zero in February at the point of harvesting, because LAI scales with height (except where deciduous behaviour is present, but this is not the case for the Miscanthus PFT).

This explanation has been added to Section 3.1:

"The seasonal cycle of growth through to harvest in mid-February is illustrated by the seasonal fluctuation of height and LAI (Figs. 2(a)-(b)."

<u>Specific comments:</u>
Page 1, Line 12: it will be better if the authors can specify the model name here rather than at line 20.

The sentence now begins "We describe developments to the land surface model JULES …"

Page 1, line 17: what is the missing model component?

Changed the text on this line from:

"…suggesting missing model components that influence growth and yields"

to:

"…primarily owing to the model's lack of representation of crop age and establishment time."

Page 2, Line 15: change "global scale" to "global scales"

Changed to "…a global scale" as I believe this is more accurate.

Page 2, Line 34: what is “TRIFFID”? You only mentioned it later.

TRIFFID was defined in this sentence, which has been rearranged for greater clarity, and now reads:

“…but these approaches have not been integrated into TRIFFID, the DGVM within JULES which links plant productivity to soil carbon and the global carbon cycle.”

Page 6, line 5: it was mentioned that “net ecosystem exchange of CO2 was measured at the Lincolnshire site”, so why not show the comparison results for NEE?

This is possible to do. However, NEE includes soil carbon respiration, which is heavily dependent on soil carbon content. The model was not specifically initialised with observed soil carbon density since soil carbon is a diagnostic variable in the model. Therefore while a comparison between observed and modelled NEE is possible, uncertainty and inconsistencies between modelled and observed soil respiration rates would prevent this analysis from providing clarity about the Miscanthus PFT.

Page 6, line 27: it will be great if the authors can specify RCP and SSP.

Reference to the CO_2 concentration corresponding to RCP2.6 now specifies RCP2.6-SSP2 derived from IMAGE. There are minor differences in CO_2 concentration between different SSPs and models within an RCP (in the SSP database https://tntcat.iiasa.ac.at/SspDb).

Page 6, line 10: what are the main soil properties you are concerned with? Do they have significant changes during the simulation period?

Soil properties are prescribed at the start of the model run and do not vary in time. They are used in the calculations of soil hydrology and thermal conductance.

Added the list of soil ancillaries in a parenthesis in Section 2.5.1.

Page 9, Line 27: it will be great if you have individual titles for the Discussion part to summarize the main findings and limitations of this study.

Separated Discussion into “Main findings and limitations” and “Further work”.

Page 11, Line 9: several other studies have implemented bioenergy crops into Earth system models. It should be the first step to get such processes implemented in JULES rather than Earth system models.

I stand by the wording used: “This is the first step to getting **such processes** represented **mechanistically** within Earth system models.”
The emphasis here is on having the relevant physical properties (such as the crop’s height at various times of the year, carbon harvested from the system at appropriate intervals) represented so we can explore the effects on the carbon cycle and climate system.

Page 11, Conclusion: can you discuss more implications of this study?

Added the following paragraph at the end of Section 5:
"Implications of this model functionality include the ability to study bioenergy cropping and harvests within a land surface model. Ultimately, this should facilitate climate change mitigation and climate modelling research to evaluate future low-carbon energy systems featuring bioenergy crops for their impacts on hydrology, climate and carbon storage."

Table 2: do you have any ranges for these parameters?

[I assume the reviewer is referring to Table 3, since Table 2 shows TRIFFID parameters and lists allowed values.]
PFT parameter choice is discussed in the Supplement and in Harper et al. (2018b).

Added this sentence to Section 2.4:
"(See also Harper et al. (2018b) for further information about PFT parameter selection.)"

Figure 4: rather than having two subplots show the observation and simulation results, could you add two more figures showing their spatial difference? Or report their spatial correlations?

The difference between modelled and observed yields has been added to Figure 4.

Review by Anonymous Referee #2 & author's response

General Comments:
The authors outline an enhancing modification of the JULES land surface model, termed JULES-BE, where BE stands for bioenergy. They describe a change to the dynamics of how cropland expands based on the assumption that new cropland will be planted, rather than being filled by the natural expansion of existing cropped area. They show that this change makes the area in bioenergy crops more faithfully conform to that prescribed by the driving IAM scenario in a 21st century simulation. They also present a PFT parameterization for the popular bioenergy crop Miscanthus. This PFT reproduces growth and structural characteristics of Miscanthus for a site in the United Kingdom but doesn't capture the the full variability of yields observed globally. The PFT also tends to predict unrealistically high yields for hot regions. They also added the ability to simulate coppice, rotation forestry, and litter harvest for bioenergy using existing woody species PFTs. They conclude the paper with demonstration forest bioenergy simulations and initial comparisons to European observations.

The authors convinced me that JULES-BE model represents a useful advancement that will help address important questions in the field. The paper is well written and outlines the technical aspects of the model clearly. I also appreciate the fact that the limitations of model and possible ways to address them are clearly identified. However, there are a few issues in the text that could be clarified or improved, which I detail below.

Specific Comments:
Section 2.2.1 (page 4, line 3):
The rationale of the 30% litter harvest assumption should be briefly described. While this is an existing model assumption the authors chose not to changed it and must therefore feel it is supported. The cited reference does not provide the reasoning for this assumption.

> Added the following explanation to Section 2.2.1:
> "Setting the harvest rate to 30 % of litter production approximates the estimate of 8.2 Pg C year^{-1} of human-appropriated net primary production from crop harvests globally in 2000 (Haberl et al., 2007). Future development of JULES-BE will allow the harvest rate to be user-prescribed for each PFT."

Section 2.5.4 (page 7, line 14):
Explain the rationale for cutting to 1 m in height.

> 1 metre height was used as an illustrative example. In short-rotation coppicing, thin stems are cut near the base from a thicker trunk, rather than to a specific height. 1 metre height equates to an above-ground biomass of 117 g C m^{-2} for *P. nigra* and 153 g C m^{-2} for *P. x euramericana*. Shorter cutting height would result in longer re-establishment times.

> The relevant sentence in section 2.5.4 has been updated and now reads:
> "Harvesting occurs on a 3-year rotation on day 270 of the year, when trees are cut to 1 metre height, allowing sufficient remaining biomass for rapid regrowth the following year."

Section 3.1 (page 7-8):

Lines 24-28: It also seems notable that the model shows onset of growth much earlier than the observations.

Agreed – this is worth mentioning.

Added this sentence to Section 3.1:
"The modelled crop also increased in height and LAI earlier in the season compared to observations."

Lines 29-30: The model underestimated the height somewhat for the simulation period (figure 2B) and slightly underestimates the observed aboveground biomass for the UK (Linchonshire) site for the modeled heights (below _2.6m, figure 2D). Given this it would seem that aboveground biomass should be low compared to observations. How then does the modeled yield exceed that at the Linconshire site by over 60%?

Added the following text to the end of Section 3.1:

"The model underestimated height during the growing season but overestimated the yields. This suggests that ratio of height to aboveground biomass was lower at this site than the sites used for calibration in Figs. 2(d) and S1. However, height at harvest time was not recorded; peak height occurred around August to September while harvest was in February or early April. It is usual for Miscanthus to lose biomass over autumn and winter; the preference for harvesting in mid/late winter is not for largest yields but for improved fuel quality and reduced nitrogen loss from the system."

Section 3.4 (page 9):
This section is underdeveloped. While the authors do make it clear that the simulations are mainly proof of principle they will be of considerable interest to many readers as they demonstrate the culmination of the model changes presented. In particular, the residue forestry panels in figure 9 are not even mentioned. These results suggest that litter harvest can provide roughly the same biomass yield as coppice while having very little impact on forest growth (comparing to the first 40 years of the rotation panels). This is a very provocative initial result and should be contextualized in the text as is done for the coppice and rotation simulations.

We will find an appropriate case in the literature to inform a new simulation of residue forestry to strengthen this proof of principle.

Section 4 (page 10):
Sentence line 22-23:
The interpretation of this sentence depends on the definition of 'crop'. Throughout the paper the term crop is used generically with section 2.4 explicitly stating "JULES-BE can represent any type of plant as a bioenergy crop" and in a few places is explicitly qualified, e.g. 'crop grasses'. Please clarify the meaning here. If the statement pertains only to annual crops like grasses I accept the conclusion. However, if trees are included in the definition of crops I would expect that the day of harvest has some potential to impact yield of short rotation coppice but will have very limited impact on predicted yield for longer forest rotations.

I agree that for forestry, altering the harvest day-of-year would have little impact on yield, but would affect other ecosystem properties. This sentence has been updated and now reads:

"Allowing harvest day-of-year to vary regionally would improve global-scale assessment of any bioenergy crop, as harvest timing is dependent on local climatology and affects local land-surface properties, such as roughness length, albedo, and transpiration rate, which in turn affect the climate."

Last paragraph starting line 26:
I am not convinced by the authors' contention that the TRIFFID completion scheme can be made to inform the choice of bioenergy crops appropriate to a given location. The authors present potential changes to the competition scheme that, if I am reading it correctly, would allow PFTs placed in the same land class to compete on the basis of aboveground biomass and / or post season yield calculations. Even if these changes were made it is not clear how this would add greater insight than performing independent simulations with potential PFTS and comparing yields directly. More fundamentally yields do not seem to be the appropriate metric for comparing bioenergy crops in the context of an ESM. If yields were the main concern species specific crop models would probably be sufficient for this purpose. While yield is certainly important for the economics of species selection, it is not sufficient for climate relevance. The value of an ESM is that it allows the impact of bioenergy crops to be examined holistically. Assessing alternatives requires considering the status of carbon stocks and biophysical feedbacks alongside the offset of emissions from crop yields. I do think JULES-BE will be useful in performing such an analysis, just not in the manner described here.

Thanks for this interesting and thoughtful critique. I do agree that the DGVM competition mechanism may never be an appropriate instrument for evaluating suitability or preferability of different BE crops in the same grid cell or bioregion.

Added the following sentence to the end of Section 4:
"Ultimately however, a yield-based competition scheme would still ignore the biophysical, economic and environmental factors that influence choice of crop type. As such, JULES-BE may always be more useful for informing these land-use decisions based on its output, rather than integrating these decisions into the existing model."

Figures 2 and S1:
Consider providing goodness of fit statistics for figure 2C, 2D, and for at least the selected model (case 1) in figure S1.

The root mean square errors of the modelled relationships to observations have been added for Case 1 of Fig S1 (all panels). These are the same relationships as in Figs. 2(c)-(d), so they have not been added to Figure 2.

Technical Corrections:
Section 2.2.2. (page 4, line 4): For consistency with the remainder of the formula litC, on both sides of the equation, should have time subscripts.

Added time subscripts to lit_c and *harvest* in Eqs. (1)-(4).

JULES-BE: representation of bioenergy crops and harvesting in the Joint UK Land Environment Simulator vn5.1

Emma W. Littleton[1,2], Anna B. Harper[2,3], Naomi E. Vaughan[4], Rebecca J. Oliver[5], Maria Carolina Duran-Rojas[2,3], Timothy M. Lenton[1,2]

[1] College of Life and Environmental Sciences, University of Exeter, Exeter, EX4 4QE, United Kingdom
[2] Global Systems Institute, University of Exeter, Exeter, EX4 4QE, United Kingdom
[3] College of Engineering, Mathematics and Physical Sciences, University of Exeter, Exeter, EX4 4QE, United Kingdom
[4] Tyndall Centre for Climate Change Research, School of Environmental Sciences, University of East Anglia, Norwich, NR4 7TJ, United Kingdom
[5] Centre for Ecology and Hydrology, Benson Lane, Wallingford, OX10 8BB, United Kingdom

Correspondence to: Emma W. Littleton (e.w.littleton@exeter.ac.uk)

Abstract. We describe developments to the~~a~~ land surface model JULES, allowing for flexible user-prescribed harvest regimes of various perennial bioenergy crops or natural vegetation types. Our aim is to integrate the most useful aspects of dedicated bioenergy models into dynamic global vegetation models, in order that assessment of bioenergy options can benefit from state-of-the-art Earth system modelling. A new plant functional type (PFT) representing *Miscanthus* is also presented. The *Miscanthus* PFT fits well with growth parameters observed at a site in Lincolnshire, UK; however, global observed yields of *Miscanthus* are far more variable than is captured by the model, ~~suggesting missing model components that influence growth and yields~~primarily owing to the model's lack of representation of crop age and establishment time. Global expansion of bioenergy crop areas under a 2 °C emissions scenario and balanced greenhouse gas mitigation strategy from the IMAGE integrated assessment model (RCP2.6-SSP2) achieves a mean yield of 4.3 billion tonnes dry matter per year over 2040–2099, around 30 % higher than the biomass availability projected by IMAGE. In addition to perennial grasses, JULES-BE can also be used to represent short-rotation coppicing; residue harvesting from cropland or forestry; and rotation forestry.

1 Introduction

A large supply of biomass energy, from diverse sources, is an essential component of most strategies to avoid dangerous climate change (Rose et al., 2013;Daioglou et al., 2019). Biomass is important both as a versatile energy source (e.g. used for heat and electricity production and transport fuels), and as part of bioenergy with carbon capture and storage (BECCS), the most feasible mechanism by which large amounts of CO_2 may be actively removed from the atmosphere (Smith et al., 2015;Bauer et al., 2017;Daioglou et al., 2019).

"Second-generation" bioenergy crops, comprising lignocellulosic perennial grasses, tree species managed as short-rotation coppice, and residues from forestry and agriculture, are the assumed preferred candidates to meet future biomass energy demand (Chum et al., 2011). They are preferred over "first-generation" biofuels such as maize and sugarcane which require higher nutrient inputs and have undesirable interactions with the food production systems (since they are food crops and must be grown on cropland) (Tilman et al., 2009).

A wide range of estimates of future bioenergy supply exists, but most 2 °C or lower scenarios feature BECCS being rolled out at scale in the next 10–20 years (Fuss et al., 2014;Clarke L. et al., 2014;Rogelj et al., 2018), with bioenergy crops delivering 100–400 EJ year^{-1} (primary energy) by 2100 (Huppmann et al., 2018). The impacts of large-scale bioenergy production on the land surface and Earth system could be significant, because changes to vegetation cover across the Earth can change climate systems through biophysical effects such as changes to albedo, evaporation and runoff, or through biogeochemical effects like disturbance or priming of soil carbon (Fontaine et al., 2004). The importance of bioenergy expansion to future efforts to limit climate change, combined with relative lack of understanding of its environmental effects, strongly motivates further efforts to improve our understanding of this process. Earth system modelling, a method by which we study many aspects of global environmental change, provides a robust framework for simulating and interrogating large-scale land use change such as bioenergy cropland expansion.

Dedicated bioenergy crop models may be used to project yields and responses to environmental stressors at site or regional level (Robertson et al., 2015). MISCANFOR (Hastings et al., 2009) is one example of a *Miscanthus* growth model that has been applied at a global scale (Pogson et al., 2013). These models tend to have simple or limited representation of soil carbon cycling, hydrology and climate. Dynamic global vegetation models (DGVMs), by contrast, are models specifically developed to address questions about large-scale vegetation patterns and productivity, and their links with the climate and Earth system (particularly as part of the Earth system models of which they form the terrestrial components) (Sitch et al., 2008). However, this typically occurs at the expense of representation of specific plant species and detailed site and management information. There are differences between DGVMs (and ESMs) in representation of bioenergy crops and calculation of harvests (Krause et al., 2018): although some ~~DGVMs and ESMs~~ feature explicit representation of bioenergy crops and harvesting (e.g. LPJml (Beringer et al., 2011;Boysen et al., 2016); ORCHIDEE-MICT-BIOENERGY (Li et al., 2018b)), others use approximations based on generic plant functional types (PFTs) and calculate harvests as a fixed proportion of productivity (e.g. NorESM (Muri, 2018)).~~.~~

Currently the Joint UK Land Environment Simulator (JULES) uses generic C3 and C4 grasses to simulate bioenergy productivity, with harvest taken from 30 % of litter (Harper et al., 2018a). In this paper, we describe new functionality developed within the JULES land surface model to represent the growth and harvest cycles of specific perennial bioenergy crops including lignocellulosic grasses (*Miscanthus*) and trees used in short-rotation coppice regimes (poplar SRC), as well as forest management (Table 1), hereafter called JULES-BE. JULES-BE represents the yield mechanistically by removing the above-ground biomass, reducing the plant's height and leaf area and allowing it to regrow. The parametrisation of a new PFT to represent *Miscanthus* is also presented. The aim of these functional developments is to simulate yields of biomass for energy feedstocks, and to evaluate the impacts of bioenergy cropping on the global carbon cycle and climate system. Therefore, this study fits best with the DGVM approach, which allows analysis of the impacts of bioenergy on climate and land surface processes. JULES has been used to model bioenergy systems before (Hughes et al., 2010;Black et al., 2012;Oliver et al., 2015), at site level, but these approaches have not been integrated into ~~JULES's DGVM,~~ TRIFFID, the DGVM within JULES which links plant productivity to soil carbon and the global carbon cycle. The improved representation of harvesting and yield we present here is unique because it facilitates the assessment of impacts of bioenergy crops on the carbon cycle and climate system in a way that has not been shown before using the JULES model.

2 Technical development

2.1 Existing model description

JULES is a community land surface model that can be run standalone (as described here) or used as the land surface component of the Met Office's Earth System models (Collins et al., 2011) . JULES is described in Best et al. (2011) and Clark et al. (2011). JULES calculates the surface energy and water fluxes, along with gross and net primary productivity, on a half-hourly or hourly time step. The net primary productivity (NPP) for each PFT is accumulated during each timestep, to be later used for calculating changes in vegetation structure and coverage in TRIFFID, the dynamic global vegetation model built into JULES. TRIFFID is called at the end of a user-defined number of days (typically 1 or 10 days), and the accumulated NPP is allocated between "growth" and "spreading." The former is used for increasing leaf area index (LAI) and canopy height, while the latter is used to allow PFTs to take up more space in a grid cell. Competition for space is determined based on PFT heights: the tallest plants get first access to space in a grid cell, but may not be able to compete if their NPP is too low.

In JULES, crops are represented in one of two ways. Major food crops such as wheat, maize and soya are represented by the JULES-crop module (Osborne et al., 2015). However, JULES-crop is suitable only for annual seed crops, and is not compatible with TRIFFID and the wider carbon cycle representation within JULES. Therefore, the TRIFFID-crop module was developed to represent crops within the carbon cycle and climate system. When the TRIFFID-crop option is enabled within JULES, multiple types of agricultural land are represented separately. The user defines the fraction of each grid cell dedicated to food crops, pasture, and bioenergy. The fractions can vary in time with new values prescribed annually or less frequently. Each of these crop area types forms a separate "land class" for which specific PFTs are allocated. TRIFFID-crop requires height-based competition (Harper et al., 2018b), which allows for a flexible number of PFTs. Each PFT is assigned to only one land class and competes only with PFTs of the same land class, within the defined fraction. Any land within the fraction that cannot be filled by the assigned PFTs is occupied by bare soil. Multiple identically parametrised PFTs may be used if the same type of plant (e.g., C3 grass) is desired in multiple land classes (e.g., natural, food crop, and pasture). TRIFFID-crop also introduces harvesting of biomass from crop areas, described in Sec. 2.2.1 as "continuous harvest". JULES-BE describes a set of options within JULES, building upon the TRIFFID-crop functionality to enable periodic harvesting and assisted expansion of bioenergy PFT area.

2.2 Harvesting regimes

Two methods of representing crop harvest are used. A new TRIFFID parameter, *harvest_type* (Table 3), may be set to 0, 1 or 2 for each PFT. A value of 0 represents no harvest; the two harvest types are described below.

2.2.1 Continuous harvest (type 1)

This harvest type is used and described by Harper et al. (2018a) and represented in Eqs. (1) and (2). A fixed percentage (currently hardcoded as 30 %) of the PFT's litter production (lit_c) is rerouted to a harvest pool ($harvest$) on a continuous basis. The remaining litter fraction (currently 70 %) enters the soil pool as normal. Setting the harvest to 30 % of litter production approximates the estimate of 8.2 Pg C $year^{-1}$ of human-appropriated net primary production from crop harvests globally in 2000 (Haberl et al., 2007). Future development of JULES-BE will allow the harvest rate to be user-prescribed for each PFT.

$$harvest_t \cancel{harvest} = 0.3 \times lit_{c_t} \cancel{lit_c} \quad (1)$$

$$lit_{c_t} \cancel{lit_c} = 0.7 \times lit_{c_t} \cancel{lit_c} \quad (2)$$

2.2.2 Periodic harvest (type 2)

At defined intervals, specified in days by the user, the PFT is reduced to a short height, also specified by the user (see Table 2 for a list of parameters). New values for wood ($woodC$), leaf ($leafC$) and root ($rootC$) biomass are calculated based on this height, per Eqs. (46, 56–58, 60) given by Clark et al. (2011) and reproduced in the Supplement. The difference between old and new above-ground carbon is allocated to the harvest pool (Eq. (3)), whereas the change in root (below-ground) carbon is added to the plant litter flux (lit_c), as given in Eq. (4). A time coefficient (Δt) is used to convert stocks to fluxes.

$$harvest_t \cancel{harvest} = \frac{(leafC_{t-1} + woodC_{t-1}) - (leafC_t + woodC_t)}{\Delta t} \quad (3)$$

$$lit_{c_t} \cancel{lit_c} = lit_{c\ t} \cancel{lit_c} + \frac{(rootC_{t-1} - rootC_t)}{\Delta t} \quad (4)$$

Since the model describes a constant perfect correlation between PFT height and balanced-growth LAI, minimum LAI must also be set low enough to accommodate the prescribed *harvest_ht* (Table 2). The PFT then begins to regrow again from its new shorter height.

2.3 Assisted expansion

This section describes new functionality which directs the model to simulate planting of new agricultural areas. In the existing scheme, when the fractional area of a land class increases, the new area is covered by bare soil, until the existing vegetation expands into it. Expansion of PFTs in the absence of competition follows Eq. (5). Equation (5) is a simplified version of Eq. (52) in Clark et al. (2011), assuming that only one PFT is assigned to the land class, the PFT occupies at least 1 % of the total grid cell, and the plant has already reached its maximum height. $Cveg$ represents the PFT's biomass density, and g_{area} is a constant parameter representing total mortality.

$$\Delta frac = frac \times \left(\frac{NPP}{Cveg} - g_{area}\right) \quad (5)$$

This arrangement represents competition and growth in natural landscapes, but where land is dedicated to a specific purpose such as bioenergy crops, it is less realistic to represent it as such; it is equivalent to humans clearing an area of land for cropping but then neglecting to plant anything.

Where the agricultural areas consist of ordinary C3 and C4 grasses, this does not pose much of a problem since $Cveg$ is usually small relative to NPP during the growing season; therefore, $\frac{NPP}{Cveg}$ can attain sufficient size to allow the grass to increase its area. The problem is more significant in the case of high-density lignocellulosic bioenergy grasses, in which NPP may be 1–3 times that of an ordinary grass but $Cveg$ is 5–10 times larger. Annual harvesting also reduces the capacity of crop grasses to increase their area, since more of their NPP is dedicated to increasing their height (i.e., one of the assumptions of Eq. (5) does not hold for much of the year).

Therefore, in order to represent the establishment of new agricultural areas, without sacrificing the benefits of dynamic vegetation, i.e. that plants can die off where the environment is unsuitable, a new planting mechanism has been implemented. This mechanism, activated using the switch *l_ag_expand* globally and the *ag_expand* switch on individual PFTs (Table 2), alters the value of $\Delta frac$ returned by TRIFFID. Land class fractions may change once per year, whereas TRIFFID (where plant competition and fractional allocation takes place) is run once per simulation day. At each grid cell, the current land class fraction is compared to the value used at the last TRIFFID call. Where the land class fraction has increased, the assisted expansion function is activated. $\Delta frac$ is calculated as it would have been without land use change ($\Delta frac_{na}$ in Eq. (6), which could be positive or negative), but then the value of the increase ($\Delta frac_{ag}$) is added to it. This is equivalent to assuming that agricultural expansion is accompanied by planting new crops. $\Delta frac$ is then added to the previous PFT fraction. If two or more PFTs (for which assisted expansion is enabled) share the same land class, the new area is divided equally between them ($NPFT_{ag}$). This process is also illustrated in Fig. 1.

$$\Delta frac = \Delta frac_{na} + \frac{\Delta frac_{ag}}{NPFT_{ag}} \quad (6)$$

2.4 New PFT parametrisation

A new bioenergy PFT was developed representing *Miscanthus*, a perennial grass of particular interest in the bioenergy literature due to its robust growth and low input requirements (Heaton et al., 2008;Zub and Brancourt-Hulmel, 2010;McCalmont et al., 2017). An earlier representation of *Miscanthus* in JULES (Hughes et al., 2010) focused on realistic representation of height and LAI, and estimated yields based on NPP. In the new method of periodic harvesting, above-ground biomass (AGB) is the most important factor determining yields, and therefore this aspect was emphasised in the development of this PFT (Fig. 2(d); Fig S1).

In the current version of JULES, around 90 PFT parameters and 13 TRIFFID parameters govern a PFT's response to its environment, although they are not all used at once because many parameters are only required by specific configurations. The *Miscanthus* PFT presented here was developed based on a generic C4 grass in the 9 PFT JULES scheme (Harper et al., 2016), with 14 parameters redefined specifically for this study. Table 3 gives an overview of the main features of the *Miscanthus* PFT. A full list of parameters and their relevance in JULES is given in the Supplement. (See also Harper et al. (2018b) for further information about PFT parameter selection.)

JULES-BE can represent any type of plant as a bioenergy crop. In addition to perennial grasses, short-rotation coppicing (SRC) with willow or poplar can be simulated, or softwood or hardwood trees for forestry (Table 1). This study introduces examples of tree types grown for biomass or bioenergy in Sec. 3.4, using two poplar PFTs developed for JULES by Oliver et al. (2015).

2.5 Methods of evaluation

Simulations were carried out to evaluate and illustrate the new functionality in JULES-BE. These simulations were all based on the JULES-ES configuration, a set of options designed for best representation of carbon cycle and climate dynamics over decadal to centennial timescales. All simulations began with initial conditions from a spin-up to equilibrium, then included a transient spin-up period prior to the main run.

2.5.1 Lincolnshire site data

Adjustment of PFT parameters for *Miscanthus* was performed using observational data collected from a commercial *Miscanthus* plantation in Lincolnshire, UK. The site is on a compacted loam soil previously used to grow wheat and oilseed rape. The site had mean annual temperature of 9.8 °C and mean annual precipitation of 621 mm. The net ecosystem exchange of CO_2 was measured by eddy covariance methodology. Gross primary productivity (GPP) was calculated using the REddyProc method described by Robertson et al. (2017), after Reichstein et al. (2005). Manual measurements of height and LAI were taken over the growing season (Fig. 2).

JULES requires meteorological and soil ancillary (time-invariant) data to drive the model. ~~was driven by m~~ Meteorological data were collected at the site on an hourly basis during 2006–2013 (shortwave and longwave radiation, wind speed, precipitation, temperature, air pressure, and specific humidity). Physical soil properties (soil albedo, heat capacity, thermal conductivity, hydraulic conductivity at saturation, soil moisture at saturation, soil moisture at critical point, soil moisture at wilting point, Brooks-Corey exponent for soil hydraulic calculations, soil matric suction at saturation) were derived from measurements taken at the site between 2009 and 2010. The site and data collection are described in greater detail by (Robertson et al., 2016;Robertson et al., 2017).

2.5.2 Global bioenergy yield dataset

In order to further explore the suitability of this *Miscanthus* PFT for simulating biomass yields, a comparison was conducted against observed yields. Li et al. (2018a) have compiled a comprehensive global dataset of bioenergy crop yields as reported in scientific literature. It includes 981 observations of *Miscanthus* yields, from the United States and Europe, with and without irrigation and fertiliser.

For comparison with modelled *Miscanthus* yields produced by JULES-BE, the observations of *Miscanthus* from this dataset were combined into 68 0.5°x0.5° grid cells. Observed sites using fertiliser or irrigation were found not to differ significantly in yield from untreated sites, and were therefore included in the comparison. (JULES-BE is not currently configured to support irrigation or nitrogen fertilisation.) JULES-BE was then run at the same 68 grid cells over the period 1980–1999, using meteorological driving data from WATCH at 0.5°x0.5° (Weedon et al., 2010;Weedon et al., 2011).

2.5.3 Future simulation

To evaluate implications of the new representation of bioenergy crops for climate mitigation, a 21st century simulation of bioenergy crop area under SSP2-RCP2.6 is shown here. Meteorological driving data from HadGEM2-ES ISIMIP simulations (for RCP2.6) were used, downscaled to 0.5° and bias-corrected to calibrate with WATCH observed climatology over 1960–1999 (Hempel et al., 2013). Atmospheric CO_2 concentrations followed the RCP2.6 CO_2 concentration pathway, covering the period 2006–2099, generated by IMAGE for SSP2. The land use scenario is generated by the IMAGE 3.0 integrated assessment model (Stehfest et al., 2014). The RCP2.6-SSP2 scenario (Doelman et al., 2018;Daioglou et al., 2019) features a rapid scale-up of global bioenergy crop area in the tropics over 2025–2045 to around 250 million hectares (Mha), followed by gradual expansion into temperate regions over the rest of the century, with fluctuations in crop area driven by bioenergy demand (Fig. 7). Figure 6, which shows yields across the global land surface, is generated using the same driving data, though bioenergy crops are not grown on all grid cells in the RCP2.6-SSP2 simulation.

2.5.4 Forestry and short-rotation coppice demonstrations

Three simulations were carried out to demonstrate the functionality of JULES-BE for harvesting of woody biomass: short-rotation coppicing (SRC); permanent (non-felling) forest management with residue harvesting; and rotation forestry plantation. They are presented as illustrative cases to inform future model development, and are thus intentionally idealised scenarios.

These three simulations were carried out for a single point, a FLUXNET site in Italy (IT-CA1, Castel d'Asso; http://sites.fluxdata.org/IT-CA1; Sabbatini et al. (2016)), at which poplar is grown on a short-rotation coppicing regime. Meteorological data was collected onsite from 2011–2014 on a half-hourly basis. Over this period, the mean annual temperature at this site was 15 °C and the mean annual precipitation was 736 mm. Site soil properties were also used. The local biome (IGBP class) is temperate deciduous forest.

All three simulations were run for a 60-year cycle, using looped meteorological driving data from 2011–14:

- Poplar SRC: two species of Poplar, *Populus nigra* and *P. x euramericana*, parametrised and evaluated by Oliver et al. (2014). Harvesting occurs on a 3-year rotation on day 270 of the year, when trees are cut to 1 metre height, allowing sufficient remaining biomass for rapid regrowth the following year. The PFT and TRIFFID parameters for the poplar PFTs are given in the Supplement.
- Residue harvesting forestry: two tree species; broadleaf deciduous tree and needleleaf evergreen tree. Generic PFT tree parameters as per Harper et al. (2018b) (reproduced in the Supplement). Continuous harvesting (50~~30~~ % of~~-~~ litter production from wood only) is applied to represent residues.
- Rotation forestry: two tree species; broadleaf deciduous tree and needleleaf evergreen tree. Generic PFT tree parameters as per Harper et al. (2018b) (reproduced in the Supplement), with *lai_min* adjusted to 0.1 to allow for harvest cutting. Harvesting occurs on a 40-year rotation on day 364 of the year, when trees are cut to 1.5 metre height.

3 Results

3.1 Lincolnshire site

Model results from the Lincolnshire site are shown in Figs. 2(a)–(c) and 3, compared against observational data from the site. The seasonal cycle of growth through to harvest in mid-February is illustrated by the seasonal fluctuation of height and LAI (Figs. 2(a)-(b)). The observations show more year-to-year variation in peak seasonal height and LAI than the model. The modelled peak heights (2.4–2.55 m during 2010–2012) and LAIs (2.75–2.9) are also generally lower than those observed (height: 2.8–3.1 m; LAI: 3.1–4.1), although observed height and LAI tended to decline after their peaks to values closer to those produced by the model. The modelled crop also increased in height and LAI earlier in the season compared to observations. The correlation between observed and modelled GPP at this site is excellent (R=0.956; Fig. 3).

The mean modelled yield was 6.0 ± 0.5 tonnes C ha^{-1} year^{-1}, equivalent to a dry matter yield of 12.4 ± 1.1 tonnes DM ha^{-1} year^{-1} assuming 48 % carbon in dry biomass (Baxter et al., 2014). This significantly exceeds the observed yields of 7.6 ± 1.6 tonnes DM ha^{-1} year^{-1} at this site (Robertson et al., 2017), though sits squarely within the range of yields observed in the UK (12.4 ± 5.9 tonnes DM ha^{-1} year^{-1}; 11 studies compiled by Li et al. (2018a)).

3.2 Modelled *Miscanthus* yields against observations

A comparison of yields was conducted between the JULES-BE model results and observed *Miscanthus* yields compiled from the literature by Li et al. (2018a). The results of this comparison are given in Figs. 4 and 5. Across all sites and years, observed yields were much more variable, with a mean ± SD of 12.5 ± 9 tonnes DM ha^{-1} $year^{-1}$ (n=981), compared to 14.3 ± 7 tonnes DM ha^{-1} $year^{-1}$ for the modelled yields (n=1360). In a few cases, yields up to 51 tonnes DM ha^{-1} $year^{-1}$ were observed, exceeding the maximum modelled yield of 37 tonnes DM ha^{-1} $year^{-1}$; but more significantly, low yields of less than four tonnes DM ha^{-1} $year^{-1}$ were much more common in the observations (Fig. 5(b)).

The modelled yields showed a consistent positive correlation with both mean annual precipitation (R=0.752) and mean annual temperature (R=0.718) (Fig. S2). For wider comparison, Fig. 6 shows simulated yields of *Miscanthus* across the global land surface. For the observed yields, the correlation with precipitation was much weaker (R=0.094), and while correlation with mean annual temperature was weak overall (R=0.252), yield appears to peak around 14–15 °C and decline with higher temperatures (Fig. S2). This difference between modelled and observed results is clearly illustrated in the southern United States, where modelled yields are as much as 20 tonnes DM ha^{-1} $year^{-1}$ higher than observations (Fig. 4). These observations were of *Miscanthus x giganteus*, a cultivar that produces very high yields in temperate climates but appears less well-adapted to high temperatures (Fedenko et al., 2013). Other perennial grasses may be more appropriate for hot climates. The model PFT would benefit from some further tuning to better represent properties such as stomatal conductance and photosynthetic temperature ~~response photosynthetic temperature~~ response, particularly the *tupp* and *vsl* parameters to better calibrate the relationship between leaf temperature and maximum rate of carboxylation of Rubisco (*Vcmax*; Sec. S1).

Figure 6 shows modelled yields for the whole Earth area, averaged over 2010–2019, in order to show the general spatial pattern of productivity of *Miscanthus*. Yields of 8–20 tonnes DM ha^{-1} $year^{-1}$ are typical for most temperate climates, increasing to a maximum of about 35 tonnes DM ha^{-1} $year^{-1}$ in the humid tropics. Yields are positively correlated with both temperature and precipitation (Fig. S2). This may help to contextualise the yields shown in Fig. 4.

3.3 Assisted expansion, global and future yields

To assess the impact of the assisted expansion feature on simulated global *Miscanthus* crop area, Fig. 7 shows total *Miscanthus* crop area in the RCP2.6-SSP2 scenario (van Vuuren et al., 2017). This scenario features a rapid increase in bioenergy crop area ("Available area"; black) from 29 Mha in 2025 to 282 Mha in 2045. "Natural expansion" (green) represents the *Miscanthus* PFT parametrised as discussed here, without using the new agricultural expansion functionality. In this scenario, *Miscanthus* occupies 13 Mha of the bioenergy crop area in 2025, increasing to 104 Mha in 2045—leaving 178 Mha as bare soil. In 2035, only 31 Mha, or 25 % of the bioenergy crop area, is occupied by *Miscanthus*. With "Assisted expansion" (blue), the *Miscanthus* PFT occupies a consistently larger proportion of the available area throughout this period of rapid increase. In 2035, the PFT covers 119 Mha, 96 % of the available area. The proportion of area covered begins to decline after 2040, as the bioenergy production area shifts from the tropics into temperate biomes which are somewhat less favourable for growth in this representation of *Miscanthus*. The difference in crop area between the old and new expansion methods declines toward the end of the simulation, as the crop area begins to stabilise and the two simulations begin to converge.

In Fig. 8, the total global *Miscanthus* yield is shown, using the “assisted expansion” method shown in Fig. 7. The bioenergy crop yield supplied in the IMAGE model is shown for reference (Huppmann et al., 2018;Doelman et al., 2018;Daioglou et al., 2019). Following the rapid increase in bioenergy crop area, from 2040-2099, bioenergy crop yields remain fairly steady in JULES-BE at 4.3 Gt DM year^{-1} globally, compared to 3.3 Gt DM year^{-1} in IMAGE over the same period. IMAGE uses a management factor when projecting energy yields, assuming that yields are currently used inefficiently (typical values are 60 % in 2020) but that improvements to crop breeding and management will increase yields to 120–140 % of physical potential by 2100 (Stehfest et al., 2014). This accounts for a portion of the gap in the early years of this scenario which closes between the two models by the 2090s. The *Miscanthus* PFT in JULES-BE probably over-estimates yields in hot climates (Fig. 4); as such, the yields projected by IMAGE may be more reliable. This scenario, and the comparison between JULES-BE and IMAGE, will be explored in greater detail in a future publication.

3.4 Demonstrations of forestry and short-rotation coppicing

Figure 9 shows illustrative simulations of short-rotation coppicing and managed forestry using JULES-BE. Over the 20 harvest cycles of poplar SRC, the yield was 2.4 ± 0.3 tonnes C ha^{-1} year^{-1} (*P. Nigra*) and 2.2 ± 0.5 tonnes C ha^{-1} year^{-1} (*P. x Euramericana*). This falls within the range observed by Sabbatini et al. (2016) over the 2011–2012 growing seasons (3.1 ± 1.5 tonnes C ha^{-1} year^{-1}) at the IT-CA1 site (growing *Populus x canadensis* on a 2-year coppicing rotation). The site received some supplemental irrigation during dry spells, which is not represented in the model; this may account for some under-estimation of yields. Residue harvesting based on wood litter produced generally small yields of 0.15–0.25 tonnes C ha^{-1} year^{-1} in addition to forest carbon stock accumulation of 45–80 tonnes C ha^{-1} over the 60-year period. For rotation forestry, the yield over the 40-year rotation was 41 t C ha^{-1} for broadleaf and 69 t C ha^{-1} for needleleaf, equivalent to 1.0 and 1.7 t C ha^{-1} year^{-1}, respectively. This is higher than the average productivity for European forests (around 0.8 t C ha^{-1} year^{-1}, assuming 250 kg C m^{-3} of harvested roundwood) (Payn et al., 2015), but lower than recent estimates from France for Douglas fir of 3.1 t C ha^{-1} year^{-1} following a 40-year rotation (Bréda and Brunette, 2019). These examples show that with appropriate tuning and validation of the PFT and harvest parameters, JULES-BE could be used to facilitate decision-making on questions such as species selection, harvesting regime, harvest frequency and timing.

4 Discussion

4.1 Main findings and limitations

Formatted: Heading 2

The modelled yields of *Miscanthus* were broadly consistent with observations from sites in the USA and Europe, but showed much less variability. A major reason for this is that the harvest frequency is fixed in the model, with no option for irregular frequency or for harvests to be skipped. For example, in practice *Miscanthus* is generally allowed 1–2 years after planting to establish before being harvested annually, followed by 1–2 years of low yields. The largest yields generally occur during years 4–10 and decline thereafter, with a typical rotation length of 20 years (Zub and Brancourt-Hulmel, 2010). In the model, there is no representation of a plant's age, so it is not possible to establish an age-dependent harvest regime. Another reason for reduced variability in yields is that the root system reverts to the same small size after each harvest (Eq. (4)), dropping its surplus biomass into the soil C pool. In reality, a relatively small proportion of root biomass is shed at harvest, and the mature plant gets a regrowth benefit from an established root system. The model currently relies on a fixed relationship between above-ground height and root biomass and breaking this link would create other problems in the model relating to PFT scaling. Future versions of JULES will use the Reduced Ecosystem Demography (RED) approach which represents separate mass classes within a PFT (Moore et al., 2018). Alternatively, an approach could be implemented similar to that of Black et al. (2012), in which three PFTs are used to represent different age classes of sugarcane, although this would not be compatible with dynamic vegetation. Given these difficulties, and the fact that JULES is a global model, accurate average yields with reduced variability compared to observations is likely to be an acceptable compromise for most applications of JULES-BE.

The *Miscanthus* PFT has not been tested with other advanced modules within TRIFFID, such as nitrogen cycling or layered soil carbon (Burke et al., 2017), and will likely require additional updating and tuning of parameters to yield useful results with other functions. Since nitrogen content is recorded for the harvested biomass, with appropriate tuning JULES-BE could also be used to quantify nitrogen loss from bioenergy crop ecosystems due to harvesting.

4.2 Further work

Formatted: Heading 2

An example of rotation forestry has been shown in Fig. 9 for a single point. To represent forestry on a country, regional or global scale, further development of the model is required. The harvest frequency and timing are currently fixed for each PFT, meaning that all grid cells are harvested at the same time. Over a large number of grid cells, this would not be realistic and would produce undesirable hydrological and climatic effects. Further improvements to the model could enable the user to stagger the timing of harvesting. Allowing harvest frequency to vary regionally would better represent rotation forestry and increase yield by enabling the user to choose a regionally appropriate harvest frequency (shorter for more productive regions). Allowing harvest day-of-year to vary regionally would improve global-scale assessment of any bioenergy crop, since harvest timing is dependent on local climatology and affects local land-surface properties, such as roughness length, albedo, and transpiration rate, which in turn affect the climate. This functionality may be best implemented by allowing these variables to be user-prescribed for each grid cell. However, providing these data may be burdensome for the user, and some predictive algorithms based on climatology and growth, built into the model, may be more appropriate.

The algorithms for competition between PFTs within TRIFFID can potentially be used to determine the most suitable type of bioenergy crop in each grid cell. However, some modifications would need to be made to the existing code. In the simulations presented in this study, TRIFFID competition was enabled, allowing the bioenergy PFT to adjust its area to scale with its productivity—for example, allowing a crop to die back in response to an unsuitable environment. The current competition scheme is not useful for allowing different types of bioenergy PFTs to compete with each other within a grid cell, since it is based on height. This favours plants that can gain height easily, rather than shorter species with greater biomass density. A competition scheme based on above-ground biomass rather than height would be the first modification to make. This could help select between species within a harvesting regime, e.g. help determine the best perennial grass for annual harvesting, or the best tree species for short-rotation coppicing. However, this may not necessarily select for the highest-yielding plant, because above-ground biomass is only a good proxy for yield at the end of the growing season, and competition for area is invoked at every iteration of TRIFFID (once per day in these simulations). Also, this development would not be useful for mixing PFTs with different harvest frequency or harvest day-of-year, since it would continue to bias competition towards the PFT that has been harvested less recently. ~~Ultimately, T~~The best solution would be to reapportion the bioenergy crop area between PFTs once per harvest cycle, based on the previous cycle's yield, but that would be a complex development given the existing model structure. Ultimately however, a yield-based competition scheme would still ignore the biophysical, economic and environmental factors that influence choice of crop type. As such, JULES-BE may always be more useful for informing these land-use decisions based on its output, rather than integrating these decisions into the existing model.

5 Conclusions

This study presents new functionality to represent second-generation bioenergy cropping and harvests in JULES. This is the first step to getting such processes represented mechanistically within Earth system models, in order that the effects of bioenergy cropping on the carbon cycle and climate system can be evaluated. JULES-BE allows for flexible parametrisation of many types of bioenergy PFTs, although only *Miscanthus* has been fully developed here. Yields of the *Miscanthus* PFT were within the range generally observed in the United States and Europe, though the model failed to capture the large variability in observed yields across and within sites.

Applications for JULES-BE include short-rotation coppicing, rotation forestry and residue harvesting from forests or agricultural systems. Future development will focus on improving the competition scheme so that multiple bioenergy PFTs can be represented simultaneously, and adding features to the harvest timing mechanism that improve representation of forest harvesting at regional or global scale.

Implications of this model functionality include the ability to study bioenergy cropping and harvests within a land surface model. Ultimately, this should facilitate climate change mitigation and climate modelling research to evaluate future low-carbon energy systems featuring bioenergy crops for their impacts on hydrology, climate and carbon storage.

Code availability. This work was based on a version of JULES5.1 with additional developments that will be included in a future release of JULES. The code is available from the JULES FCM repository: https://code.metoffice.gov.uk/trac/jules (registration required). The version used was r12164_biotiles_harvest (located in the repository at branches/dev/emmalittleton/r12164_biotiles_harvest).

Author contributions. The aims and objectives of the project were jointly developed by EWL, ABH, NEV and TML. EWL developed the model code with help from ABH and MCDR and designed and performed the validation simulations with advice from ABH, NEV, RJO and TML. EWL and ABH prepared the manuscript with contributions from NEV, RJO, MCDR and TML.

Competing interests. The authors declare that they have no competing interests.

Acknowledgements. This work is part of FAB GGR (Feasibility of Afforestation and Biomass energy with carbon capture and storage for Greenhouse Gas Removal), a project funded by the UK Natural Environment Research Council (NE/P019951/1), part of a wider Greenhouse Gas Removal research programme (http://www.fab-ggr.org/). EWL and ABH also acknowledge support from the UK EPSRC Fellowship EP/N030141/1. MCDR acknowledges support from the CRESCENDO projects that received funding from the European Union's Horizon 2020 research and innovation program under grant number agreement No 641816. Thanks are due to Jon Finch for carrying out the data collection at the Lincolnshire *Miscanthus* site. The authors thank Eddy Robertson and Andy Wiltshire for providing consultation and advice on the model development. Thanks also to Sarah Chadburn for feedback on draft figures. Maps were produced using map data from naturalearthdata.com.

References

Amougou, N., Bertrand, I., Cadoux, S., and Recous, S.: Miscanthus × giganteus leaf senescence, decomposition and C and N inputs to soil, GCB Bioenergy, 4, 698-707, https://doi.org/10.1111/j.1757-1707.2012.01192.x, 2012.

Bauer, N., Calvin, K., Emmerling, J., Fricko, O., Fujimori, S., Hilaire, J., Eom, J., Krey, V., Kriegler, E., Mouratiadou, I., Sytze de Boer, H., van den Berg, M., Carrara, S., Daioglou, V., Drouet, L., Edmonds, J. E., Gernaat, D., Havlik, P., Johnson, N., Klein, D., Kyle, P., Marangoni, G., Masui, T., Pietzcker, R. C., Strubegger, M., Wise, M., Riahi, K., and van Vuuren, D. P.: Shared Socio-Economic Pathways of the Energy Sector – Quantifying the Narratives, Glob. Environ. Change, 42, 316-330, https://doi.org/10.1016/j.gloenvcha.2016.07.006, 2017.

Baxter, X. C., Darvell, L. I., Jones, J. M., Barraclough, T., Yates, N. E., and Shield, I.: Miscanthus combustion properties and variations with Miscanthus agronomy, Fuel, 117, 851-869, https://doi.org/10.1016/j.fuel.2013.09.003, 2014.

Beringer, T. I. M., Lucht, W., and Schaphoff, S.: Bioenergy production potential of global biomass plantations under environmental and agricultural constraints, GCB Bioenergy, 3, 299-312, https://doi.org/10.1111/j.1757-1707.2010.01088.x, 2011.

Best, M. J., Pryor, M., Clark, D. B., Rooney, G. G., Essery, R. L. H., Ménard, C. B., Edwards, J. M., Hendry, M. A., Porson, A., Gedney, N., Mercado, L. M., Sitch, S., Blyth, E., Boucher, O., Cox, P. M., Grimmond, C. S. B., and Harding, R. J.: The Joint UK Land Environment Simulator (JULES), model description – Part 1: Energy and water fluxes, Geoscientific Model Development, 4, 677-699, https://doi.org/10.5194/gmd-4-677-2011, 2011.

Black, E., Vidale, P. L., Verhoef, A., Cuadra, S. V., Osborne, T., and Van den Hoof, C.: Cultivating C4 crops in a changing climate: sugarcane in Ghana, Environ. Res. Lett., 7, https://doi.org/10.1088/1748-9326/7/4/044027, 2012.

Boysen, L. R., Lucht, W., Gerten, D., and Heck, V.: Impacts devalue the potential of large-scale terrestrial CO2 removal through biomass plantations, Environmental Research Letters, 11, https://doi.org/10.1088/1748-9326/11/9/095010, 2016.

Bréda, N., and Brunette, M.: Are 40 years better than 55? An analysis of the reduction of forest rotation to cope with drought events in a Douglas fir stand, Ann. For. Sci., 76, https://doi.org/10.1007/s13595-019-0813-3, 2019.

Burke, E. J., Chadburn, S. E., and Ekici, A.: A vertical representation of soil carbon in the JULES land surface scheme (vn4.3_permafrost) with a focus on permafrost regions, Geosci. Model Dev., 10, 959-975, https://doi.org/10.5194/gmd-10-959-2017, 2017.
Christian, D. G., Riche, A. B., and Yates, N. E.: Growth, yield and mineral content of Miscanthus × giganteus grown as a biofuel for 14 successive harvests, Ind. Crop Prod., 28, 320-327, https://doi.org/10.1016/j.indcrop.2008.02.009, 2008.
Chum, H., A. Faaij, J. Moreira, G. Berndes, P. Dhamija, H. Dong, B. Gabrielle, A. Goss Eng, W. Lucht, M. Mapako, O. Masera Cerutti, T. McIntyre, T. Minowa, and Pingoud, K.: Bioenergy, in: IPCC Special Report on Renewable Energy Sources and Climate Change Mitigation, edited by: O. Edenhofer, R. Pichs-Madruga, Y. Sokona, K. Seyboth, P. Matschoss, S. Kadner, T. Zwickel, P. Eickemeier, G. Hansen, S. Schlömer, and Stechow, C. v., Cambridge University Press, Cambridge, United Kingdom and New York, NY, USA, 209-332, 2011.
Clark, D. B., Mercado, L. M., Sitch, S., Jones, C. D., Gedney, N., Best, M. J., Pryor, M., Rooney, G. G., Essery, R. L. H., Blyth, E., Boucher, O., Harding, R. J., Huntingford, C., and Cox, P. M.: The Joint UK Land Environment Simulator (JULES), model description – Part 2: Carbon fluxes and vegetation dynamics, Geosci. Model Dev., 4, 701-722, https://doi.org/10.5194/gmd-4-701-2011, 2011.
Clarke L., K. Jiang, K. Akimoto, M. Babiker, G. Blanford, K. Fisher-Vanden, J.-C. Hourcade, V. Krey, E. Kriegler, A. Löschel, D. McCollum, S. Paltsev, S. Rose, P. R. Shukla, M. Tavoni, B. C. C. van der Zwaan, and Vuuren, D. P. v.: Assessing Transformation Pathways, in: Climate Change 2014: Mitigation of Climate Change. Contribution of Working Group III to the Fifth Assessment Report of the Intergovernmental Panel on Climate Change, edited by: Edenhofer, O., R. Pichs-Madruga, Y. Sokona, E. Farahani, S. Kadner, K. Seyboth, A. Adler, I. Baum, S. Brunner, P. Eickemeier, B. Kriemann, J. Savolainen, S. Schlömer, C. von Stechow, Zwickel, T., and Minx, J. C., Cambridge University Press, Cambridge, United Kingdom and New York, NY, USA, 413-510, 2014.
Collins, W. J., Bellouin, N., Doutriaux-Boucher, M., Gedney, N., Halloran, P., Hinton, T., Hughes, J., Jones, C. D., Joshi, M., Liddicoat, S., Martin, G., O'Connor, F., Rae, J., Senior, C., Sitch, S., Totterdell, I., Wiltshire, A., and Woodward, S.: Development and evaluation of an Earth-System model – HadGEM2, Geosci. Model Dev., 4, 1051-1075, https://doi.org/10.5194/gmd-4-1051-2011, 2011.
Cosentino, S. L., Patanè, C., Sanzone, E., Copani, V., and Foti, S.: Effects of soil water content and nitrogen supply on the productivity of Miscanthus × giganteus Greef et Deu. in a Mediterranean environment, Ind. Crop Prod., 25, 75-88, https://doi.org/10.1016/j.indcrop.2006.07.006, 2007.
Daioglou, V., Doelman, J. C., Wicke, B., Faaij, A., and van Vuuren, D. P.: Integrated assessment of biomass supply and demand in climate change mitigation scenarios, Glob. Environ. Change, 54, 88-101, https://doi.org/10.1016/j.gloenvcha.2018.11.012, 2019.
Doelman, J. C., Stehfest, E., Tabeau, A., van Meijl, H., Lassaletta, L., Gernaat, D. E. H. J., Hermans, K., Harmsen, M., Daioglou, V., Biemans, H., van der Sluis, S., and van Vuuren, D. P.: Exploring SSP land-use dynamics using the IMAGE model: Regional and gridded scenarios of land-use change and land-based climate change mitigation, Glob. Environ. Change, 48, 119-135, https://doi.org/10.1016/j.gloenvcha.2017.11.014, 2018.
Fedenko, J. R., Erickson, J. E., Woodard, K. R., Sollenberger, L. E., Vendramini, J. M. B., Gilbert, R. A., Helsel, Z. R., and Peter, G. F.: Biomass Production and Composition of Perennial Grasses Grown for Bioenergy in a Subtropical Climate Across Florida, USA, BioEnerg. Res., 6, 1082-1093, https://doi.org/10.1007/s12155-013-9342-3, 2013.
Feng, X. P., Chen, Y., Qi, Y. H., Yu, C. L., Zheng, B.-S., Brancourt-Hulmel, M., and Jiang, D.-A.: Nitrogen enhanced photosynthesis of Miscanthus by increasing stomatal conductance and phosphoenolpyruvate carboxylase concentration, Photosynthetica, 50, 577-586, https://doi.org/10.1007/s11099-012-0061-3, 2012.
Fontaine, S., Bardoux, G., Abbadie, L., and Mariotti, A.: Carbon input to soil may decrease soil carbon content, Ecol. Lett., 7, 314-320, https://doi.org/10.1111/j.1461-0248.2004.00579.x, 2004.
Fuss, S., Canadell, J. G., Peters, G. P., Tavoni, M., Andrew, R. M., Ciais, P., Jackson, R. B., Jones, C. D., Kraxner, F., Nakicenovic, N., Le Quéré, C., Raupach, M. R., Sharifi, A., Smith, P., and Yamagata, Y.: Betting on negative emissions, Nat. Clim. Change, 4, 850-853, https://doi.org/10.1038/nclimate2392, 2014.
Haberl, H., Erb, K. H., Krausmann, F., Gaube, V., Bondeau, A., Plutzar, C., Gingrich, S., Lucht, W., and Fischer-Kowalski, M.: Quantifying and mapping the human appropriation of net primary production in earth's terrestrial ecosystems, Proceedings of the National Academy of Sciences, 104, 12942, https://doi.org/10.1073/pnas.0704243104, 2007.

Harper, A. B., Cox, P. M., Friedlingstein, P., Wiltshire, A. J., Jones, C. D., Sitch, S., Mercado, L. M., Groenendijk, M., Robertson, E., Kattge, J., Bönisch, G., Atkin, O. K., Bahn, M., Cornelissen, J., Niinemets, Ü., Onipchenko, V., Peñuelas, J., Poorter, L., Reich, P. B., Soudzilovskaia, N. A., and van Bodegom, P.: Improved representation of plant functional types and physiology in the Joint UK Land Environment Simulator (JULES v4.2) using plant trait information, Geosci. Model Dev., 9, 2415-2440, https://doi.org/10.5194/gmd-9-2415-2016, 2016.

Harper, A. B., Powell, T., Cox, P. M., House, J., Huntingford, C., Lenton, T. M., Sitch, S., Burke, E., Chadburn, S. E., Collins, W. J., Comyn-Platt, E., Daioglou, V., Doelman, J. C., Hayman, G., Robertson, E., van Vuuren, D., Wiltshire, A., Webber, C. P., Bastos, A., Boysen, L., Ciais, P., Devaraju, N., Jain, A. K., Krause, A., Poulter, B., and Shu, S.: Land-use emissions play a critical role in land-based mitigation for Paris climate targets, Nat. Commun., 9, 2938, https://doi.org/10.1038/s41467-018-05340-z, 2018a.

Harper, A. B., Wiltshire, A. J., Cox, P. M., Friedlingstein, P., Jones, C. D., Mercado, L. M., Sitch, S., Williams, K., and Duran-Rojas, C.: Vegetation distribution and terrestrial carbon cycle in a carbon cycle configuration of JULES4.6 with new plant functional types, Geosci. Model Dev., 11, 2857-2873, https://doi.org/10.5194/gmd-11-2857-2018, 2018b.

Hastings, A., Clifton-Brown, J., Wattenbach, M., Mitchell, C. P., and Smith, P.: The development of MISCANFOR, a new Miscanthus crop growth model: towards more robust yield predictions under different climatic and soil conditions, GCB Bioenergy, 1, 154-170, https://doi.org/10.1111/j.1757-1707.2009.01007.x, 2009.

Heaton, E. A., Dohleman, F. G., and Long, S. P.: Meeting US biofuel goals with less land: the potential of Miscanthus, Glob. Change Biol., 14, 2000-2014, https://doi.org/10.1111/j.1365-2486.2008.01662.x, 2008.

Hempel, S., Frieler, K., Warszawski, L., Schewe, J., and Piontek, F.: Bias corrected GCM input data for ISIMIP Fast Track, GFZ Data Services, https://doi.org/http://doi.org/10.5880/PIK.2016.001, 2013.

Hughes, J. K., Lloyd, A. J., Huntingford, C., Finch, J. W., and Harding, R. J.: The impact of extensive planting of Miscanthus as an energy crop on future CO2 atmospheric concentrations, GCB Bioenergy, 2, 79-88, https://doi.org/10.1111/j.1757-1707.2010.01042.x, 2010.

Huppmann, D., Kriegler, E., Krey, V., Riahi, K., Rogelj, J., Rose, S. K., Weyant, J., Bauer, N., Bertram, C., Bosetti, V., Calvin, K., Doelman, J., Drouet, L., Emmerling, J., Frank, S., Fujimori, S., Gernaat, D., Grubler, A., Guivarch, C., Haigh, M., Holz, C., Iyer, G., Kato, E., Keramidas, K., Kitous, A., Leblanc, F., Liu, J.-Y., Löffler, K., Luderer, G., Marcucci, A., McCollum, D., Mima, S., Popp, A., Sands, R. D., Sano, F., Strefler, J., Tsutsui, J., Van Vuuren, D., Vrontisi, Z., Wise, M., and Zhang, R.: IAMC 1.5°C Scenario Explorer and Data hosted by IIASA, Integrated Assessment Modeling Consortium & International Institute for Applied Systems Analysis, https://doi.org/10.22022/SR15/08-2018.15429, 2018.

Jeżowski, S., Głowacka, K., and Kaczmarek, Z.: Variation on biomass yield and morphological traits of energy grasses from the genus Miscanthus during the first years of crop establishment, Biomass Bioenergy, 35, 814-821, https://doi.org/10.1016/j.biombioe.2010.11.013, 2011.

Krause, A., Pugh, T. A. M., Bayer, A. D., Li, W., Leung, F., Bondeau, A., Doelman, J. C., Humpenoder, F., Anthoni, P., Bodirsky, B. L., Ciais, P., Muller, C., Murray-Tortarolo, G., Olin, S., Popp, A., Sitch, S., Stehfest, E., and Arneth, A.: Large uncertainty in carbon uptake potential of land-based climate-change mitigation efforts, Glob. Change Biol., 24, 3025-3038, https://doi.org/10.1111/gcb.14144, 2018.

LeBauer, D., Kooper, R., Mulrooney, P., Rohde, S., Wang, D., Long, S. P., and Dietze, M. C.: BETYdb: a yield, trait, and ecosystem service database applied to second-generation bioenergy feedstock production, GCB Bioenergy, 10, 61-71, https://doi.org/10.1111/gcbb.12420, 2018.

Li, W., Ciais, P., Makowski, D., and Peng, S.: A global yield dataset for major lignocellulosic bioenergy crops based on field measurements, Sci. Data, 5, 180169, https://doi.org/10.1038/sdata.2018.169, 2018a.

Li, W., Yue, C., Ciais, P., Chang, J., Goll, D., Zhu, D., Peng, S., and Jornet-Puig, A.: ORCHIDEE-MICT-BIOENERGY: an attempt to represent the production of lignocellulosic crops for bioenergy in a global vegetation model, Geosci. Model Dev., 11, 2249-2272, https://doi.org/10.5194/gmd-11-2249-2018, 2018b.

McCalmont, J. P., Hastings, A., McNamara, N. P., Richter, G. M., Robson, P., Donnison, I. S., and Clifton-Brown, J.: Environmental costs and benefits of growing Miscanthus for bioenergy in the UK, GCB Bioenergy, 9, 489-507, https://doi.org/10.1111/gcbb.12294, 2017.

Moore, J. R., Zhu, K., Huntingford, C., and Cox, P. M.: Equilibrium forest demography explains the distribution of tree sizes across North America, Environ. Res. Lett., 13, https://doi.org/10.1088/1748-9326/aad6d1, 2018.

Muri, H.: The role of large—scale BECCS in the pursuit of the 1.5°C target: an Earth system model perspective, Environ. Res. Lett., 13, https://doi.org/10.1088/1748-9326/aab324, 2018.
Oliver, R. J., Blyth, E., Taylor, G., and Finch, J. W.: Water use and yield of bioenergy poplar in future climates: modelling the interactive effects of elevated atmospheric CO2 and climate on productivity and water use, GCB Bioenergy, 7, 958-973, https://doi.org/10.1111/gcbb.12197, 2015.
Osborne, T., Gornall, J., Hooker, J., Williams, K., Wiltshire, A., Betts, R., and Wheeler, T.: JULES-crop: a parametrisation of crops in the Joint UK Land Environment Simulator, Geosci. Model Dev., 8, 1139-1155, https://doi.org/10.5194/gmd-8-1139-2015, 2015.
Payn, T., Carnus, J.-M., Freer-Smith, P., Kimberley, M., Kollert, W., Liu, S., Orazio, C., Rodriguez, L., Silva, L. N., and Wingfield, M. J.: Changes in planted forests and future global implications, Forest Ecol. Manag., 352, 57-67, https://doi.org/10.1016/j.foreco.2015.06.021, 2015.
Pogson, M., Hastings, A., and Smith, P.: How does bioenergy compare with other land-based renewable energy sources globally?, GCB Bioenergy, 5, 513-524, https://doi.org/10.1111/gcbb.12013, 2013.
Reichstein, M., Falge, E., Baldocchi, D., Papale, D., Aubinet, M., Berbigier, P., Bernhofer, C., Buchmann, N., Gilmanov, T., Granier, A., Grunwald, T., Havrankova, K., Ilvesniemi, H., Janous, D., Knohl, A., Laurila, T., Lohila, A., Loustau, D., Matteucci, G., Meyers, T., Miglietta, F., Ourcival, J.-M., Pumpanen, J., Rambal, S., Rotenberg, E., Sanz, M., Tenhunen, J., Seufert, G., Vaccari, F., Vesala, T., Yakir, D., and Valentini, R.: On the separation of net ecosystem exchange into assimilation and ecosystem respiration: review and improved algorithm, Glob. Change Biol., 11, 1424-1439, https://doi.org/10.1111/j.1365-2486.2005.001002.x, 2005.
Robertson, A. D., Davies, C. A., Smith, P., Dondini, M., and McNamara, N. P.: Modelling the carbon cycle of Miscanthus plantations: existing models and the potential for their improvement, GCB Bioenergy, 7, 405-421, https://doi.org/10.1111/gcbb.12144, 2015.
Robertson, A. D., Davies, C. A., Smith, P., Stott, A. W., Clark, E. L., and McNamara, N. P.: Carbon Inputs from Miscanthus Displace Older Soil Organic Carbon Without Inducing Priming, BioEnerg. Res., 10, 86-101, https://doi.org/10.1007/s12155-016-9772-9, 2016.
Robertson, A. D., Whitaker, J., Morrison, R., Davies, C. A., Smith, P., and McNamara, N. P.: A Miscanthus plantation can be carbon neutral without increasing soil carbon stocks, GCB Bioenergy, 9, 645-661, https://doi.org/10.1111/gcbb.12397, 2017.
Rogelj, J., D. Shindell, K. Jiang, S. Fifita, P. Forster, V. Ginzburg, C. Handa, H. Kheshgi, S. Kobayashi, E. Kriegler, L. Mundaca, R. Séférian, and Vilariño, M. V.: Mitigation Pathways Compatible with 1.5°C in the Context of Sustainable Development, in: Global Warming of 1.5°C. An IPCC Special Report on the impacts of global warming of 1.5°C above pre-industrial levels and related global greenhouse gas emission pathways, in the context of strengthening the global response to the threat of climate change, sustainable development, and efforts to eradicate poverty edited by: Masson-Delmotte, V., P. Zhai, H.-O. Pörtner, D. Roberts, J. Skea, P.R. Shukla, A. Pirani, W. Moufouma-Okia, C. Péan, R. Pidcock, S. Connors, J.B.R. Matthews, Y. Chen, X. Zhou, M.I. Gomis, E. Lonnoy, T. Maycock, M. Tignor, and T. Waterfield, In Press, 93-174, 2018.
Rose, S. K., Kriegler, E., Bibas, R., Calvin, K., Popp, A., van Vuuren, D. P., and Weyant, J.: Bioenergy in energy transformation and climate management, Climatic Change, 123, 477-493, https://doi.org/10.1007/s10584-013-0965-3, 2013.
Sabbatini, S., Arriga, N., Bertolini, T., Castaldi, S., Chiti, T., Consalvo, C., Njakou Djomo, S., Gioli, B., Matteucci, G., and Papale, D.: Greenhouse gas balance of cropland conversion to bioenergy poplar short-rotation coppice, Biogeosciences, 13, 95-113, https://doi.org/10.5194/bg-13-95-2016, 2016.
Sitch, S., Huntingford, C., Gedney, N., Levy, P. E., Lomas, M., Piao, S. L., Betts, R., Ciais, P., Cox, P., Friedlingstein, P., Jones, C. D., Prentice, I. C., and Woodward, F. I.: Evaluation of the terrestrial carbon cycle, future plant geography and climate-carbon cycle feedbacks using five Dynamic Global Vegetation Models (DGVMs), Glob. Change Biol., 14, 2015-2039, https://doi.org/10.1111/j.1365-2486.2008.01626.x, 2008.
Smith, P., Davis, S. J., Creutzig, F., Fuss, S., Minx, J., Gabrielle, B., Kato, E., Jackson, R. B., Cowie, A., Kriegler, E., van Vuuren, D. P., Rogelj, J., Ciais, P., Milne, J., Canadell, J. G., McCollum, D., Peters, G., Andrew, R., Krey, V., Shrestha, G., Friedlingstein, P., Gasser, T., Grübler, A., Heidug, W. K., Jonas, M., Jones, C. D., Kraxner, F., Littleton, E., Lowe, J., Moreira, J. R., Nakicenovic, N., Obersteiner, M., Patwardhan, A., Rogner, M., Rubin, E., Sharifi, A., Torvanger, A., Yamagata, Y., Edmonds, J., and Yongsung, C.: Biophysical and economic limits to negative CO2 emissions, Nat. Clim. Change, 6, 42, https://doi.org/10.1038/nclimate2870, 2015.

Stehfest, E., van Vuuren, D., Kram, T., Bouwman, L., Alkemade, R., Bakkenes, M., Biemans, H., Bouwman, A., den Elzen, M., Janse, J., Lucas, P., , van Minnen, J., Müller, C., and Prins, A.: Integrated Assessment of Global Environmental Change with IMAGE 3.0. Model description and policy applications, PBL Netherlands Environmental Assessment Agency, The Hague, 2014.

Tilman, D., Socolow, R., Foley, J. A., Hill, J., Larson, E., Lynd, L., Pacala, S., Reilly, J., Searchinger, T., Somerville, C., and Williams, R.: Beneficial Biofuels—The Food, Energy, and Environment Trilemma, Science, 325, 270, https://doi.org/10.1126/science.1177970, 2009.

van Vuuren, D. P., Stehfest, E., Gernaat, D. E. H. J., Doelman, J. C., van den Berg, M., Harmsen, M., de Boer, H. S., Bouwman, L. F., Daioglou, V., Edelenbosch, O. Y., Girod, B., Kram, T., Lassaletta, L., Lucas, P. L., van Meijl, H., Müller, C., van Ruijven, B. J., van der Sluis, S., and Tabeau, A.: Energy, land-use and greenhouse gas emissions trajectories under a green growth paradigm, Glob. Environ. Change, 42, 237-250, https://doi.org/10.1016/j.gloenvcha.2016.05.008, 2017.

Weedon, G. P., Gomes, S., Viterbo, P., Österle, H., Adam, J. C., Bellouin, N., Boucher, O., and Best, M. J.: The WATCH Forcing Data 1958–2001: a meteorological forcing dataset for land surface- and hydrological models, WATCH Tech. Rep. 22, available at: www.eu-watch.org/, 2010.

Weedon, G. P., Gomes, S., Viterbo, P., Shuttleworth, W. J., Blyth, E., Österle, H., Adam, J. C., Bellouin, N., Boucher, O., and Best, M.: Creation of the WATCH Forcing Data and Its Use to Assess Global and Regional Reference Crop Evaporation over Land during the Twentieth Century, J. Hydrometeorol., 12, 823-848, https://doi.org/10.1175/2011JHM1369.1, 2011.

Zub, H. W., and Brancourt-Hulmel, M.: Agronomic and physiological performances of different species of Miscanthus, a major energy crop. A review, Agron. Sustain. Dev., 30, 201-214, https://doi.org/10.1051/agro/2009034, 2010.

Table 1. Functionality and applications of JULES-BE.

Function	Simulated applications
Continuous harvest	Forest management (without felling)
	Biomass removal from agricultural land
Periodic harvest	Harvests of perennial crops (e.g. *Miscanthus*)
	Short rotation coppicing (e.g. poplar)
	Forestry rotations
Assisted expansion	Planting out of new agricultural areas with bioenergy crops or trees

Table 2. TRIFFID parameters required for JULES-BE. An explanation of the use of these parameters is given in Sec. 2.2.

Parameter	Type	Values	Definition
crop	integer	0	Natural land
		1	Food crop
		2	Pasture
		3	Bioenergy crops
harvest_type	integer	0	No harvest
		1	Continuous harvest
		2	Periodic harvest
harvest_freq	integer	0	Placeholder for harvest types 0 or 1
		>0	Interval in days between harvests
harvest_doy	integer	0	Placeholder for harvest types 0 or 1
		>0	Day of year on which harvest takes place
harvest_ht	real	0	Placeholder for harvest types 0 or 1
		>0	Height to which crop is reduced on harvest [metres]
ag_expand	integer	0	No automatic increase of PFT fraction when land class fraction increases
		1	Automatically plant out new crop areas with target PFTs

Table 3. PFT parameters distinguishing the *Miscanthus* PFT used in this study. "C4 Grass" parameters are taken from (Harper et al., 2018b); "*Miscanthus* (Hughes)" are given by Hughes et al. (2010). A full list of parameters, with definitions and explanations for values used, is given in the Supplement. "-" indicates parameters that were not yet introduced in the older version of JULES used by Hughes et al. (2010). Parameters described as "Allometry" were determined via an iterative process to improve the relationships between above-ground biomass, leaf area index (LAI) and height, as described in the Supplement. Parameters described as "BETYdb" were taken from observations in the Biofuel Ecophysiological Traits and Yields database (LeBauer et al., 2018). "GPP calibration" indicates *tlow* was determined via an iterative process to improve the fit of modelled gross primary productivity (GPP) to the flux data obtained from the Lincolnshire site. "Litter calibration" indicates *g_leaf_0* was determined via an iterative process to approximate the observed ratio of leaf litter to yield (Amougou et al., 2012). Details of these calculations are provided in the Supplement.

Parameter	C4 Grass (Harper)	*Miscanthus* (Hughes)	*Miscanthus* (this study)	Rationale
a_wl	0.005	0.014	0.07	Allometry
a_ws	1	0.9	1	Non-woody plant (100 % live stem)
alpha	0.04	0.067	0.067	Hughes et al. (2010)
b_wl	1.667	1.667	2	Allometry
eta_sl	0.01	0.01	0.08	Allometry
lma	0.137	-	0.065	Feng et al. (2012)
tlow	13	7.85	12.8	GPP calibration
lai_max	3	3	10	BETYdb
lai_min	1	0.6	0.1	LAI at minimum height (*harvest_ht* = 0.1)
nmass	0.0113	-	0.0217	BETYdb
nr	0.0084	-	0.0228	BETYdb
nsw	0.0202	-	0.0101	BETYdb
g_leaf_0	3	-	2	Litter calibration

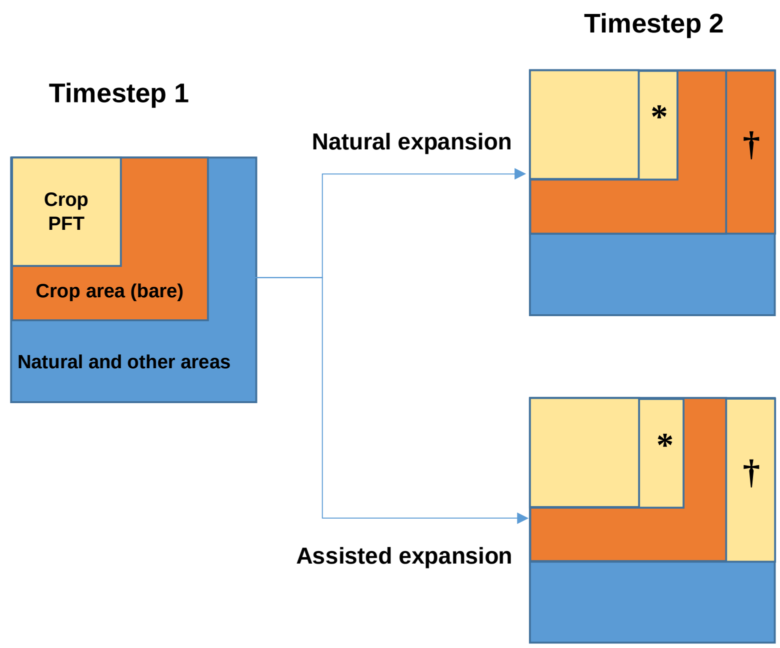

Figure 1. Schematic of the agricultural expansion functionality in JULES-BE. A full description of the process is provided in Sec. 2.3. The area marked * represents the change in the plant functional type (PFT) area that would occur without the change in crop area ($\Delta frac_{na}$ in Eq. (6)). The area marked with † represents the newly available agricultural area ($\Delta frac_{ag}$ in Eq. (6)), which is immediately populated with the crop PFT where assisted expansion is enabled, or left bare where it is disabled.

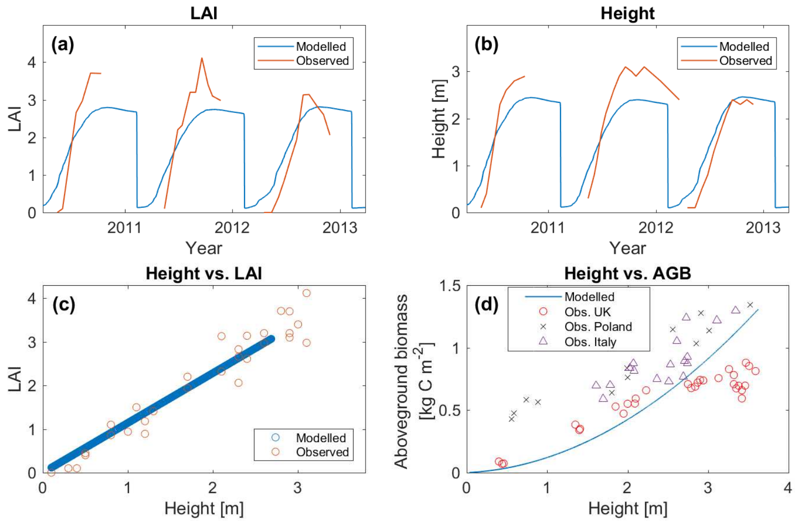

Figure 2: (a) and (b): Modelled leaf area index (LAI) and height of *Miscanthus*, compared against observations at Lincolnshire, UK, for the period 2010–2013. (c) Relationship between height and LAI, model compared against observations at Lincolnshire, UK. (d) Relationship between height and above-ground biomass (AGB), generic equation from model compared against observations from the UK (Christian et al., 2008), Poland (Jeżowski et al., 2011) and Italy (Cosentino et al., 2007).

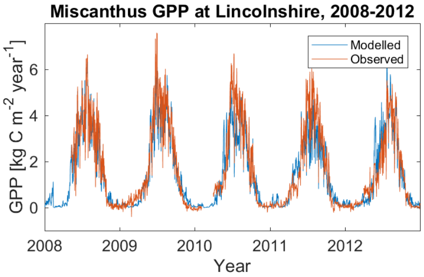

Figure 3. Modelled gross primary productivity of *Miscanthus*, compared against observations at Lincolnshire, UK, for the period 2008–2012.

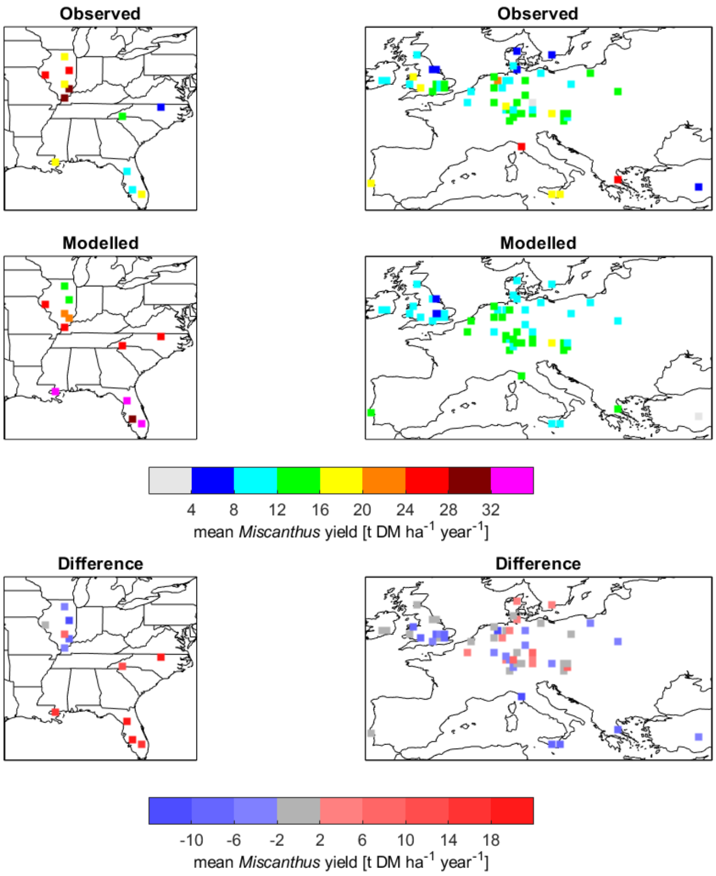

Figure 4. Comparison of modelled *Miscanthus* yields against observations from Li et al. (2018a).

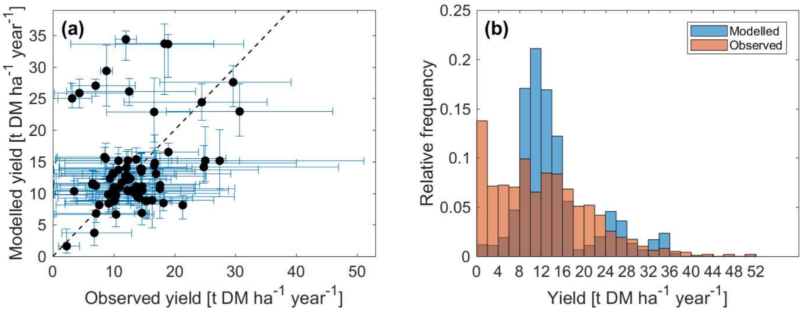

Figure 5. Modelled yields compared to observed yields of *Miscanthus* collated by Li et al. (2018a). In (a), the error bars give the range of data at each half-degree grid cell. The observed range (horizontal error bars) accounts for variation between sites (different sites may exist within a grid cell area), years, and fertiliser or irrigation treatment; the modelled range (vertical error bars) reflects interannual variability only. (b) shows the range of values by relative frequency. This figure may be compared to Fig. 3(e)–(f) from Li et al. (2018b).

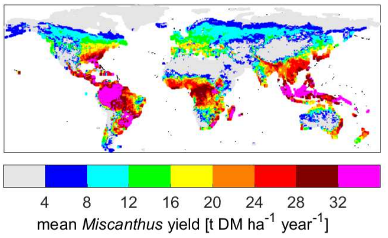

Figure 6. Modelled yields of the *Miscanthus* PFT, averaged over 2010–2019.

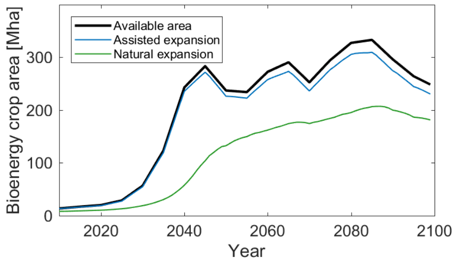

Figure 7. Modelled area of *Miscanthus* under RCP2.6-SSP2, showing the effect of the agricultural expansion functionality. "Assisted expansion" shows the model run using the assisted expansion function, compared to "Natural expansion" in which this function is disabled. "Available area" shows the total available area for bioenergy crops under this scenario.

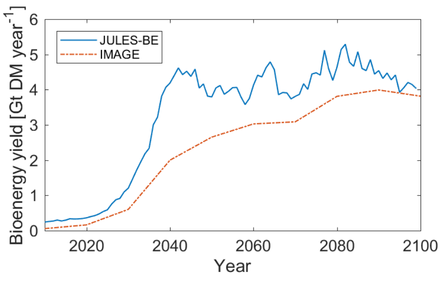

Figure 8. Bioenergy crop yield from *Miscanthus* under the land-use scenario RCP2.6-SSP2, compared to equivalent bioenergy yield in IMAGE (Huppmann et al., 2018).

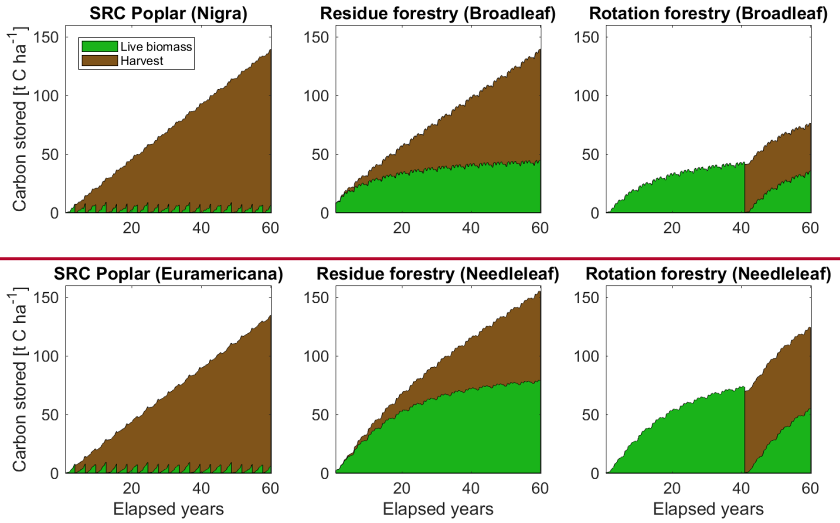
SRC Poplar (Nigra)
Residue forestry (Broadleaf)
Rotation forestry (Broadleaf)
SRC Poplar (Euramericana)
Residue forestry (Needleleaf)
Rotation forestry (Needleleaf)
Live biomass
Harvest
Carbon stored [t C ha^{-1}]
Elapsed years
0
50
100
150
20
40
60

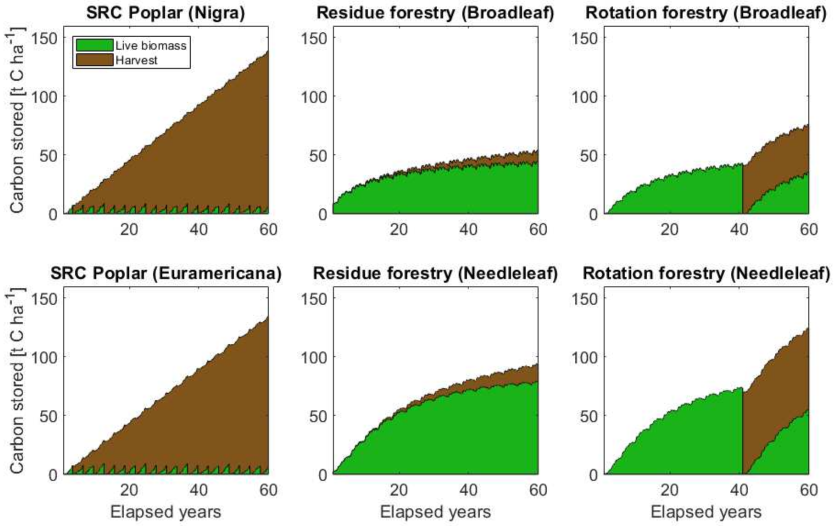
SRC Poplar (Nigra)
Residue forestry (Broadleaf)
Rotation forestry (Broadleaf)
SRC Poplar (Euramericana)
Residue forestry (Needleleaf)
Rotation forestry (Needleleaf)
Live biomass
Harvest
Carbon stored [t C ha^{-1}]
Elapsed years
0
50
100
150
20
40
60

Figure 9. Illustrated cumulative harvests and vegetation regrowth over a 60-year period, showing the application of JULES-BE to short rotation coppicing (left); permanent forestry with harvest of wood litter (middle), and rotation forestry (right).

Supplement to: JULES-BE: representation of bioenergy crops and harvesting in the Joint UK Land Environment Simulator vn5.1

Emma W. Littleton, Anna B. Harper, Naomi E. Vaughan, Rebecca J. Oliver, Maria Carolina Duran-Rojas, Timothy M. Lenton

S1. *Miscanthus* PFT parametrisation

The *Miscanthus* PFT presented here was developed based on a generic C4 grass in the 9 PFT JULES scheme (Harper et al. 2016), with six parameters taken from Hughes et al. (2010), and nine parameters redefined specifically for this study. A full list of PFT and TRIFFID parameters for all bioenergy PFTs used in this study is given in the Supplementary spreadsheet.

Since the periodic harvest mechanism described in this study harvests from above-ground biomass, the chief focus of PFT tuning has been to improve representation of above-ground biomass (AGB).

Five parameters define the allometry of the PFT, i.e. the relationship between height, leaf area index (LAI), and mass of respective portions of the PFT:

- A_{ws}: ratio of total stem biomass to live stem biomass. For all non-woody plants (defined here as grasses), this ratio is equal to 1, meaning that all stem biomass is alive and respiring.
- A_{wl}: wood-to-leaf scaling parameter relating total stem biomass to LAI.
- *LMA*: Leaf mass per area [kg leaf m^{-2} per unit of LAI].
- B_{wl}: allometric exponent relating stem biomass to LAI.
- Eta_{sl}: Ratio of live stem biomass to LAI.

The scaling of the plant is derived iteratively at each TRIFFID call, beginning with L_b (balanced-growth LAI). Absent of deciduous behaviour, L_b is always equal to actual LAI. L_b is bounded by *lai_min* and *lai_max*, which are defined in TRIFFID parameters.

After L_b is determined at each TRIFFID call, the three PFT biomass components are calculated per Equations (56), (57) and (58) in Clark et al. 2011. All units are kg C m^{-2}.

$$Leaf = L_b \times LMA \times 0.4 \quad \text{(S1)}$$

$$Root = Leaf \quad \text{(S2)}$$

$$Wood = A_{wl} \times {L_b}^{B_{wl}} \quad \text{(S3)}$$

$$Cveg = Leaf + Root + Wood \quad \text{(S4)}$$

$$AGB = Leaf + Wood \quad \text{(S5)}$$

PFT height, *canht*, is related to wood biomass as per Eq. (61) in Clark et al. 2011:

$$canht = \frac{Wood}{A_{ws} \times Eta_{sl}} \times \left(\frac{A_{wl}}{Wood}\right)^{1/B_{wl}} \quad \text{(S6)}$$

Using the equation above for relating *Wood* to *Lb*, this simplifies to:

$$canht = \frac{a_{wl} \times {L_b}^{b_{wl}-1}}{a_{ws} \times \eta_{sl}} \quad \text{(S7)}$$

Above-ground biomass thus relates to L_b:

$$AGB = a_{wl} \times {L_b}^{b_{wl}} + L_b \times LMA \times 0.4 \quad \text{(S8)}$$

In tuning this PFT, *LMA* was fixed at 0.065 kg m^{-2} (Feng et al. 2012), and A_{ws} fixed to 1 in common with other "non-woody" PFTs. The remaining free parameters therefore are A_{wl}, B_{wl}, and Eta_{sl}. The default values for C4 grasses are A_{wl}=0.005, B_{wl}=1.667, and Eta_{sl}=0.01.

Height:AGB, Height:LAI, and Height:(stem proportion of AGB) were calculated using a range of values for A_{wl}, B_{wl}, and Eta_{sl}, a total of 600 parameter combinations.

- A_{wl}: 0.01-0.1 in increments of 0.01
- B_{wl}: 1.333-3 in increments of 0.333
- Eta_{sl}: 0.01-0.1 in increments of 0.01

Observed height:AGB relationships were combined from Cosentino et al. (2007), Jezowski et al. (2011), and Christian et al. 2008 (n=57). Height:LAI relationships were taken from the Lincolnshire site (Fig. 2) (n=15) (Robertson et al, 2016, 2017). Height:stem proportion observations were taken from Cosentino et al. (2007) (n=18). Where two y-values (AGB, LAI or stem%) were given for the same height, the mean of the y-values was taken for that height. The given sample sizes already reflect the mean of repeated x-values. Stem proportion is calculated as (wood)/(AGB) at harvest time.

These relationships (height:AGB, height:LAI, height:stem proportion) were compared against observations, and the root mean square error (RMSE) calculated for each of the parameter combinations for each relationship.

Five "cases" were selected from the 600 parameter combinations, representing the lowest combined RMSE; the lowest combined RMSE of AGB and LAI (prioritised for accuracy over stem proportion); and the lowest RMSE from each of AGB, LAI, and stem proportion independently. Figure S1 shows how height relates to AGB, LAI, and stem proportion under each of these cases. Case 1 was selected as the parametrisation that provides the best fit to AGB while providing reasonable values for LAI and stem proportion.

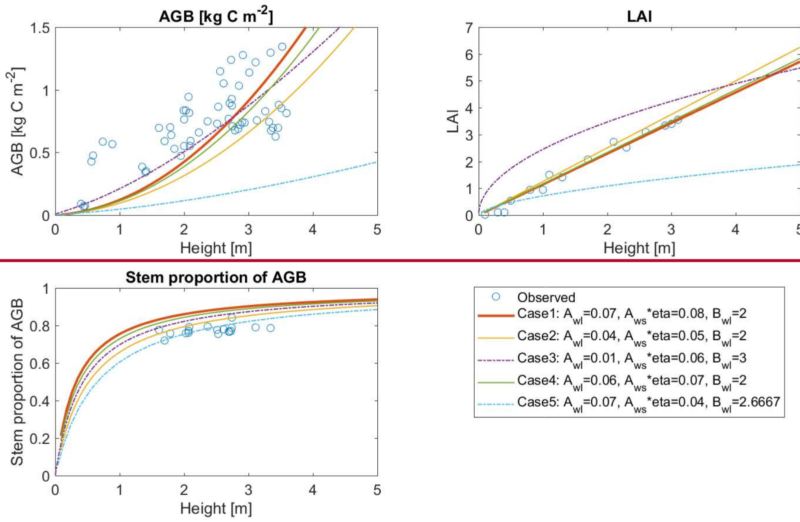

AGB [kg C m-2]
LAI
Stem proportion of AGB
AGB [kg C m-2]
LAI
Stem proportion of AGB
Height [m]
Height [m]
Height [m]
Observed
Case1: Awl=0.07, Aws*eta=0.08, Bwl=2
Case2: Awl=0.04, Aws*eta=0.05, Bwl=2
Case3: Awl=0.01, Aws*eta=0.06, Bwl=3
Case4: Awl=0.06, Aws*eta=0.07, Bwl=2
Case5: Awl=0.07, Aws*eta=0.04, Bwl=2.6667

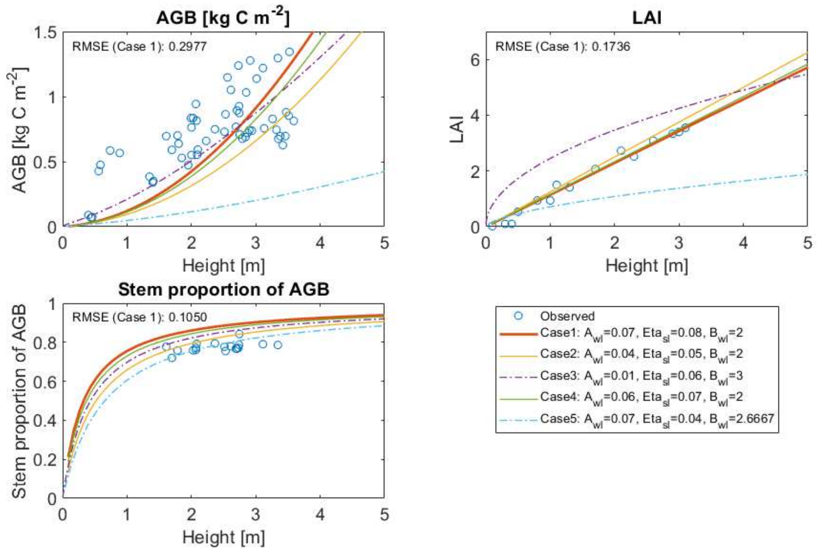

Figure S1. Fitting of allometric parameters A_{wl}, Eta_{sl} and B_{wl} to observations of aboveground biomass (AGB), leaf area index (LAI) and stem proportion of aboveground biomass. AGB observations are combined from Christian et al. (2008); Cosentino et al. (2007); Jezowski et al. (2011). LAI observations are collected from the Lincolnshire site (Robertson et al. 2016/7). Stem proportion observations are from Cosentino et al. (2007).

Gross primary productivity, respiration and litter production

Canopy assimilation depends on three limiting rates of leaf photosynthesis. For C4 plants, these are a light-limited rate, a limitation from PEPCarboxylase, and a Rubisco-limited rate (Collatz et al., 1992;Clark et al., 2011). With adequate light, the maximum rate of carboxylation of Rubisco (V_{cmax}) limits photosynthesis. The V_{cmax} is a bell-shaped function of canopy temperature, dependent on PFT parameters T_{upp} and T_{low}, and the standardised value of V_{cmax} at 25°C ($V_{cmax,25}$), which is modelled as a linear function of leaf N per unit area (N_{area}):

$$V_{cmax,25} = V_{int} + V_{sl} \times N_{area} \tag{S9}$$

Where

$$N_{area} = LMA * N_{mass} \tag{S10}$$

N_{mass} is the leaf N per unit mass (kg N (kg leaf)$^{-1}$). For C4 grasses, the default values of LMA, N_{mass}, T_{upp} and T_{low} are 0.137, 0.0113, 45 and 13, respectively, which yield an optimal V_{cmax} of 74 μmol CO_2 m^{-2} s^{-1} at 41°C.

Plant nitrogen content affects the gross primary productivity (GPP), plant respiration, and therefore total biomass (C_{veg}). Values for N_{mass} (kg N (kg leaf)$^{-1}$), N_r (N:C ratio of roots) and N_{sw} (N:C ratio of stem wood) were determined for *Miscanthus* using values from BETYdb (LeBauer et al., 2018), and assuming carbon concentration of dry biomass of 40 % for leaves and roots (hardcoded in JULES for all PFTs) and 48 % for stems (after Baxter et al., 2014). The value of T_{low} was tested iteratively against GPP measurements at the Lincolnshire site from 2008-2012 until further iterations failed to reduce the root mean square error. New values of *LMA*, N_{mass}, and T_{low} (0.065 kg m^{-2}, 0.0217 kg kg^{-1} and 12.8 °C, respectively) resulted in a lower optimal V_{cmax} of 67 µmol CO_2 m^{-2} s^{-1} at 41°C.

N_r and N_{sw} were changed from 0.0084 and 0.0202, respectively, (default values for C4 grasses) to 0.0228 and 0.0101. These changes (along with the increased Eta_{sl}) result in slightly higher root N and stem N that is four times higher than for C4 grasses. In other words, the larger woody content of *Miscanthus* comes at a cost in terms of the maintenance respiration, since in JULES maintenance respiration is a function of plant N content (Harper et al., 2018b).

The leaf turnover rate, *gleaf_0*, represents mean lifetime in years of a leaf absent of any climate-deciduous behaviour. Observations from Amougou et al. (2012) revealed cumulative leaf litter of 13–15 % as much as above-ground biomass at harvest time. Absent deciduous behaviour, leaf litter production is linearly correlated to LAI, but *gleaf* is only one of the factors; the equation is:

$$leaf_{litc} = gleaf \times LMA \times LAI \times 0.4 \tag{S10}$$

$$LAI = \frac{leaf_{litc}}{gleaf \times LMA \times 0.4} \tag{S11}$$

$$AGB = a_{wl} \times \left(\frac{leaf_{litc} \times 0.4 \times LMA}{gleaf}\right)^{b_{wl}} + \frac{leaf\_litc}{gleaf} \tag{S12}$$

Given the values above for a_{wl}, LMA, b_{wl}, Eq. (S12) simplifies to:

$$AGB = 0.07 \times \left(\frac{leaf_{litc} \times 0.026}{gleaf}\right)^2 + \frac{leaf_{litc}}{gleaf} \tag{S13}$$

gleaf was adjusted iteratively until annual *leaf_litc* at the Lincolnshire site reached 15 % of AGB at harvest, at *gleaf* = 2.

S2. Response of *Miscanthus* yield to climatic variables in model and observations

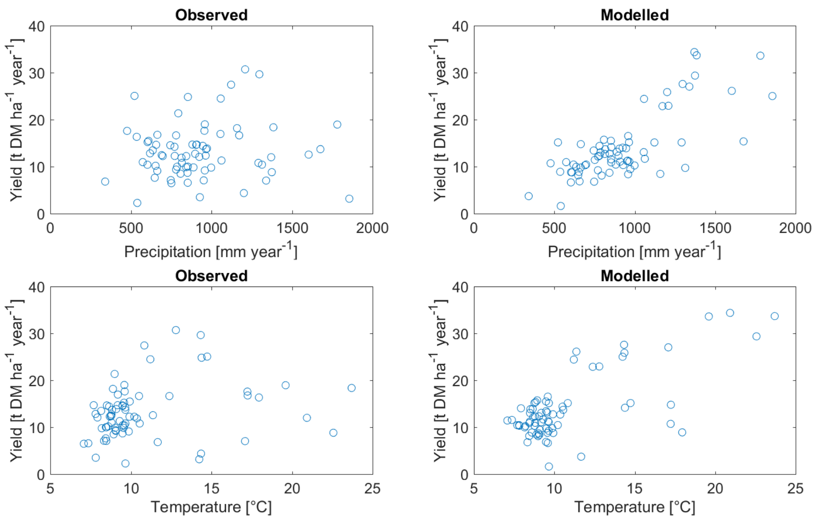

Figure S2. Relationship of observed (left) and modelled (right) *Miscanthus* yields to mean annual precipitation (top) and mean annual temperature (bottom). Precipitation and temperature were both derived from WATCH meteorological forcing data over the model simulation period (1980–1999).

S3. Growth characteristics for *Miscanthus* and C4 grass

Formatted: Heading 1

Formatted: Font: Italic

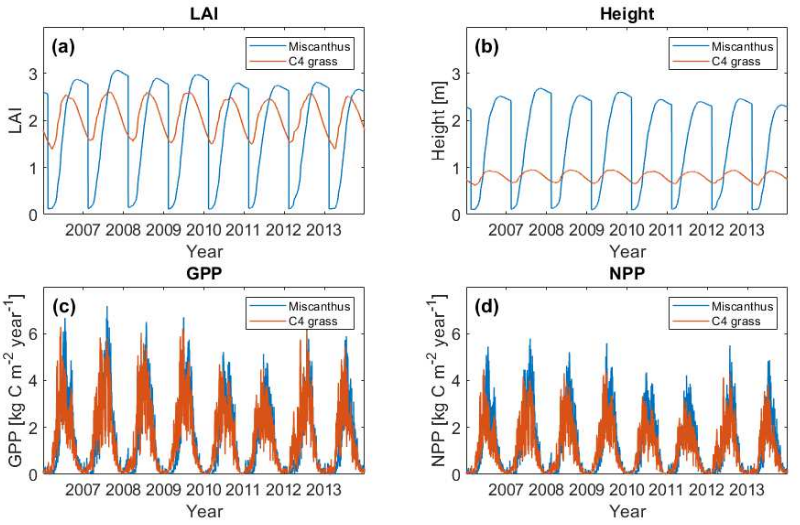

Figure S3: Modelled leaf area index (LAI), height, gross primary productivity (GPP) and net primary productivity (NPP) for the Miscanthus PFT compared to the generic C4 grass PFT, over the period 2006-2013 at the Lincolnshire site.

Formatted: Caption

References

Amougou, N., Bertrand, I., Cadoux, S., and Recous, S.: Miscanthus × giganteus leaf senescence, decomposition and C and N inputs to soil, GCB Bioenergy, 4, 698-707, https://doi.org/10.1111/j.1757-1707.2012.01192.x, 2012.

Baxter, X. C., Darvell, L. I., Jones, J. M., Barraclough, T., Yates, N. E., and Shield, I.: Miscanthus combustion properties and variations with Miscanthus agronomy, Fuel, 117, 851-869, https://doi.org/10.1016/j.fuel.2013.09.003, 2014.

Christian, D. G., Riche, A. B., and Yates, N. E.: Growth, yield and mineral content of Miscanthus × giganteus grown as a biofuel for 14 successive harvests, Ind. Crop Prod., 28, 320-327, https://doi.org/10.1016/j.indcrop.2008.02.009, 2008.

Clark, D. B., Mercado, L. M., Sitch, S., Jones, C. D., Gedney, N., Best, M. J., Pryor, M., Rooney, G. G., Essery, R. L. H., Blyth, E., Boucher, O., Harding, R. J., Huntingford, C., and Cox, P. M.: The Joint UK Land Environment Simulator (JULES), model description – Part 2: Carbon fluxes and vegetation dynamics, Geosci. Model Dev., 4, 701-722, https://doi.org/10.5194/gmd-4-701-2011, 2011.

Collatz, G. J., Ribas-Carbo, M., and Berry, J. A.: Coupled photosynthesis-stomatal conductance model for leaves of C4 plants, Aust. J. Plant Physiol., 19, 519–538, 1992.

Cosentino, S. L., Patanè, C., Sanzone, E., Copani, V., and Foti, S.: Effects of soil water content and nitrogen supply on the productivity of Miscanthus × giganteus Greef et Deu. in a Mediterranean environment, Ind. Crop Prod., 25, 75-88, https://doi.org/10.1016/j.indcrop.2006.07.006, 2007.

Feng, X. P., Chen, Y., Qi, Y. H., Yu, C. L., Zheng, B.-S., Brancourt-Hulmel, M., and Jiang, D.-A.: Nitrogen enhanced photosynthesis of Miscanthus by increasing stomatal conductance and phosphoenolpyruvate carboxylase concentration, Photosynthetica, 50, 577-586, https://doi.org/10.1007/s11099-012-0061-3, 2012.

Harper, A. B., Cox, P. M., Friedlingstein, P., Wiltshire, A. J., Jones, C. D., Sitch, S., Mercado, L. M., Groenendijk, M., Robertson, E., Kattge, J., Bönisch, G., Atkin, O. K., Bahn, M., Cornelissen, J., Niinemets, Ü., Onipchenko, V., Peñuelas, J., Poorter, L., Reich, P. B., Soudzilovskaia, N. A., and van Bodegom, P.: Improved representation of plant functional types and physiology in the Joint UK Land Environment Simulator (JULES v4.2) using plant trait information, Geosci. Model Dev., 9, 2415-2440, https://doi.org/10.5194/gmd-9-2415-2016, 2016.

Harper, A. B., Wiltshire, A. J., Cox, P. M., Friedlingstein, P., Jones, C. D., Mercado, L. M., Sitch, S., Williams, K., and Duran-Rojas, C.: Vegetation distribution and terrestrial carbon cycle in a carbon cycle configuration of JULES4.6 with new plant functional types, Geosci. Model Dev., 11, 2857-2873, https://doi.org/10.5194/gmd-11-2857-2018, 2018b.

Hughes, J. K., Lloyd, A. J., Huntingford, C., Finch, J. W., and Harding, R. J.: The impact of extensive planting of Miscanthus as an energy crop on future CO2 atmospheric concentrations, GCB Bioenergy, 2, 79-88, https://doi.org/10.1111/j.1757-1707.2010.01042.x, 2010.

Jeżowski, S., Głowacka, K., and Kaczmarek, Z.: Variation on biomass yield and morphological traits of energy grasses from the genus Miscanthus during the first years of crop establishment, Biomass and Bioenergy, 35, 814-821, https://doi.org/10.1016/j.biombioe.2010.11.013, 2011.

LeBauer, D., Kooper, R., Mulrooney, P., Rohde, S., Wang, D., Long, S. P., and Dietze, M. C.: BETYdb: a yield, trait, and ecosystem service database applied to second-generation bioenergy feedstock production, GCB Bioenergy, 10, 61-71, https://doi.org/10.1111/gcbb.12420, 2018.

Robertson, A. D., Whitaker, J., Morrison, R., Davies, C. A., Smith, P., and McNamara, N. P.: A Miscanthus plantation can be carbon neutral without increasing soil carbon stocks, GCB Bioenergy, 9, 645-661, https://doi.org/10.1111/gcbb.12397, 2017.